COMPARISON OF MECHANICAL PROPERTIES OF HYDROXYAPATITE DERIVED FROM DIFFERENT ADDITIVE POWDERS WITH CONVENTIONAL SINTERING

SEE KWAN WERN

**FACULTY OF ENGINEERING
UNIVERSITY OF MALAYA
KUALA LUMPUR**

2018

COMPARISON OF MECHANICAL PROPERTIES OF HYDROXYAPATITE DERIVED FROM DIFFERENT ADDITIVE POWDERS WITH CONVENTIONAL SINTERING

SEE KWAN WERN

THESIS SUBMITTED IN FULFILMENT OF THE REQUIREMENTS FOR THE DEGREE OF MASTER IN ENGINEERING (MANUFACTURING)

FACULTY OF ENGINEERING
UNIVERSITY OF MALAYA
KUALA LUMPUR

2018

ABSTRACT

Hydroxyapatite powder was prepared by wet chemical precipitation using eggshells derived CaO and H_3PO_4. The effects of calcination of temperature on the purity of CaO extracted from waste eggshells were investigated from 700°C to 1000°C. XRD results show the formation of pure CaO with highest purity achieved at 900°C. Hence, a calcination temperature of 900°C was chosen to produce CaO. The hydroxyapatite powder obtained after precipitation was milled together with 0.5% wt additive of Zinc Oxide, Magnesium Oxide, Aluminum Oxide and Titanium Oxide for evaluated the mechanical and physical properties. The sintering temperature for these samples ranged from 1050°C to 1350°C. It was perceived that at sintering temperature from 1050°C to 1250°C, all the additive doped HA samples demonstrated better hardness and fracture toughness than undoped HA. The maximum Vickers hardness was at 1250°C for all the additives, the fractures toughness showed better results at 1150°C. At a sintering temperature of 1350°C, the hardness and toughness decreased. This is suspected to be due to the decomposition of HA to its secondary phases (α-TCP and TTCP) and hence reducing its performance. Among all the sintering additive, aluminum oxide shows the best performance for hardness and fracture toughness. The hardness of Aluminum oxide (Al_2O_3) doped HA peaked at 1250°C (7.551GPa) and the fracture toughness of Al_2O_3 doped HA peaked at a maximum value (1.35 MPam$^{1/2}$) when sintered at 1150°C.

.

ABSTRAK

Hydroxyapatite (HA) disediakan dengan kaedah pemendakan kimia basah melalui sisa kulit telur , CaO dan H_3PO_4. Kesan suhu pensinteran diselidik dari 700 °C hingga 1000 °C supaya dapat memperolehi keaslian CaO daripada sisa kilit telur. Berdasarkan keputusan XRD, keaslian CaO diperolehi pada 900°C. Dengan itu, suhu pensinteran sebanyak 900°C dipilih bagi menghasiklkan CaO. Serbuk hydroxyapatite yang diperolehi selepas pemendakan kimia basah akan dikisar bersama dengan 0.5% wt Zink Oksida, Magnesium Oksida, Aluminium Oksida dan Titanium Oksida untuk menilai sifat mekanikal dan fizikal. Suhu pensinteran untuk semua sampel adalah dari 1050 °C hingga 1350 °C. Berdasarkan keputusan pensinteran dari 1050 °C hingga 1250 °C, semua sample aditif menunjukkan kekerasan yang lebih baik dan ketangguhan retak daripada HA yang tanpa aditif. Kekerasan Vickers menunjukkan maksimum pada 1250 °C untuk semua aditif manakala ketangguhan retak menunjukkan keputusan yang lebih baik pada 1150 °C. Pada suhu pensinteran 1350 ° C, kekerasan dan ketangguhan retak menunjukkan hala menurun. Ini disebabkan oleh pereputan HA ke fasa kedua (α-TCP dan TTCP) dan dengan itu mengurangkan prestasinya. Di antara semua aditif pensiteran, aluminium oksida menunjukkan prestasi yang terbaik untuk kekerasan dan ketangguhan retak. Kekerasan aluminium oksida (Al_2O_3) menunjukkan prestasi yang terbaik pada 1250 °C (7.551GPa) dan ketangguhan retak Al_2O_3 mencapai pada nilai maksimum (1.35 MPam$^{1/2}$) apabila disinter pada suhu 1150 ° C.

ACKNOWLEDGEMENTS

I would like to express my sincere appreciation to the following individuals that have constantly guided and supported me throughout the course of my master research:

1. My project supervisor, Associate Prof. Dr. Hendrik Simon Cornelis Metselaar for his vital encouragement, support, knowledge transfers and constructive suggestions throughout the research and the thesis writing.

2. Mr Amir Reza Akhiani, postgraduate student to help me throughout my research and guide me until complete this project.

3. Mr Tauqik, Lab Assistant at ceramic lab to guide me on the procedure for certain experiments.

4. My colleagues University of Malaya for their immeasurable guidance and advices.

I also dedicate my dissertation work to my family. I hope that this achievement will complete the dream that you had for me all those many years ago when you chose to give me the best education you could.

TABLE OF CONTENTS

LIST OF FIGURES

LIST OF TABLES

LIST OF SYMBOLS AND ABBREVIATIONS

p	:	Bulk Density
α-TCP	:	Alpha-Tricalcium Phosphate
Al_2O_3	:	Alumina
BET	:	Brunauer-Emmett-Teller
C_4P	:	Tetracalcium Phosphate
$Ca(OH)_2$	:	Calcium Hydroxide
Ca/P	:	Calcium to Phosphorous Ratio
$Ca_{10}(PO_4)_6(OH)_2$	:	Calcium Phosphate Tribasic / Hydroxyapatite
FTIR	:	Fourier Transform Infrared
H_3PO_4	:	Orthophosphoric Acid
HA	:	Hydroxyapatite
H_v	:	Vickers Hardness
KI_c	:	Fracture Toughness
NH_3	:	Ammonia
NH_4OH	:	Ammonium Hydroxide
OH	:	Hydroxyl
SBF	:	Simulated Body Fluid
SEM	:	Scanning Electron Microscope
SiC	:	Silicon Carbide
TCP	:	Tricalcium Phosphate
TEM	:	Transmission Electron Microscope
TTCP	:	Tetracalcium Phosphate
ZnO	:	Zinc Oxide
TiO_2	:	Titanium Oxide
MgO	:	Magnesium Oxide
β-TCP	:	Beta-Tricalcium Phosphate

LIST OF APPENDICES

CHAPTER 1: INTRODUCTION

1.1 INTRODUCTION TO BIOCERAMICS

The ceramics which are used in the reconstruction of a deteriorated muscular-skeletal system are classified as bio-ceramics. These materials serve as joint or tissue replacement, as well as coating in metallic implants to improve biocompatibility (Jayaswal et al., 2010). Bio- ceramic can be further categorized into bio-inert, bio-active and bio-resorbable ceramic (Hench, 1991). Examples of materials based on is classification are highlighted in Table 1.1. Bio-active materials generally exhibit biological behavior at the interface of the material where bonds between the material and tissues are formed (Hench, 1991). In contrast, bio-inert materials result in the formation of non-adherent fibrous layers on its surface, indicating a poor response of the host tissue to the material (Best et al.,2008). On the other hand, bio-resorbable ceramics act as a temporary framework and promote the growth of newly formed tissues into defected sites, before dissolving in a physiological environment (Dorozhkin, 2009; Jayaswal et al., 2010).

Table 1.1: Classification and examples of various bio-ceramics. (Best et al.,2008; Chevalier & Gremillard, 2009; Hench, 1991)

Classification	Material
Bio-active	Hydroxyapatite/Bio-glass/Glass ceramic
Bio-resorbable	Tricalcium phosphate (TCP)
Bio-inert	Alumina/Zirconia

The evolution of bio-ceramics began with the development of inert materials, where the primary aim was to substitute natural bone. This then progressed to the second generation which aimed to enhance the bioactivity of the material while trying to achieve mechanical properties similar to that of natural bone. Finally, the third generation of bio-ceramics has

to do with the development of an adequate scaffolding system which allows the hard tissue to perform its natural course (Vallet-Regi, 2010)

Alumina and zirconia are regarded as bio-inert materials which are primarily used to fabricate femoral heads. Even though these materials have high mechanical strength and outstanding wear resistance, they are generally isolated in the body due to their foreign nature. As such the bonding of alumina and zirconia implants to the bone structure is considered to be impossible (Jayaswal et al, 2010; Vallet-Regi, 2010). On the other hand, glass ceramics and bio-glass are both bio-active and have high mechanical strength. Both these materials are primarily based on silica (SiO_2). The bonding mechanisms occur when a hydrated layer is formed on the glass surface due to the leaching of alkali from the glass. This then promotes the growth of a calcium phosphate layer on the glass which acts as a bond between the newly formed bone and the glass (Doremus, 2991; Jayaswal et al,.2010). Different compositions of SiO_2 translate to varying bonding compatibility to bone. SiO_2 compositions lower than 60 wt% generally enhance bone bonding, whereas beyond this point, bone bonding is ineffective. (Best et al.,2008; Doremus, 1992)

Hydroxyapatite (HA) has the ability to integrate with bone structure besides supporting bone ingrowth without degradation. However, its poor mechanical properties limit its usage to non-load bearing applications. Therefore, it is commonly used in bone defect filling, middle ear surgery, coating of metallic implants and dental applications (Dorozhkinm 2009). Nevertheless, the ability of HA to form indistinguishable unions with bone, apart from its ability to rapidly integrate with the human body highlights its- superiority as a bio-active ceramic compared to other materials (Jayaswal et al.,2010) Examples of bio-resorbable ceramics are tricalcium phosphate (TCP), such as α-TCP an β-TCP. These

materials are highly dissolvable and are commonly used in bone cements, scaffolds and composites for bone repair. (Carrodeguas & De Aza, 2011)

1.2 HYDROSYAPATITE (HA) FROM BIOGENIC RESOURCE

As individuals age, osteoblast cells begin to degenerate, leading to a decrease in bone density, indirectly corresponding to a deterioration in the human strength. Consequently, the reduction in strength can result in fractured bones, spinal complications or even collapsed vertebrae (Dorozhkin, 2010). A solution to the aforementioned bone defects lies in bone grafting, which over the years has become a preferred option in terms of bone defect reconstruction. Being similar to the bone structure options in terms of its mineral composition as well as its highly biocompatible and bioactive nature. Hydroxyapatite (HA) has made its mark in the medical and health related field as a candidate material for the development of endosseous implants (Best et al., 2008; Ramesh et al.,2007a; Tsend et al., 2009; Zhou & Lee, 2011).

Autografts, Allografts and Xenografts are also used to treat bone related trauma and fractures (Mondal et al., 2012). Autograft tissues are regarded as a benchmark for bone grafting, however the high risks invoved such as thrombosis, blood loss, increase in morbidity as well as post-operative pain, deters its usage as a bone graft (Ben-Nissan, 2003; Ooi et al., 2007). The limitation in terms of the quantity of autogenous bone graft that can be harvested from the patient has led to the usage of Allografts. However, due to its low osteogenicity and the risk of transmission of disease such as HIV and Hepatitis, its usage is limited in the medical practice. Xenografts on the other hand, are advantageous as it is similar in structure and morphology to the human bone, but the presence of pathogens can

potentially be harmful to the patient. Calcination at elevated temperature is able to destroy these pathogens. (Ben-Nissan, 2003: Ooi et al.,2007)

Due to the limitation of the mentioned bone graft, the need for bone like implants is as compelling as ever. Studies have shown that the human bone is similar in terms of its chemical composition to carbonated HA (CHA) rather than stoichiometric HA (Bigi et al.,1997; Marten et al.,2010; Vallet-Regi & Gonzalez-Calbet,2004).

Experimental studies conducted on CHA have shown to enhance biocompatibility (Eles et al, 1988; Landi et al., 2003) and being highly soluble in nature, CHA is capable of increase bioactivity (Patel et al., 2002; Porter et al., 2003). HA derived from natural resources and bio waste such a bovine bone, porcine bone, fishbone, cuttlefish bone and coral are capable to producing CHA. This is an attractive alternative in the production of biomedical implants (Ben-Nissan, 2003; Boutinguiza et al., 2012, Figueitredo et al., 2010; Milovac et al.,2014; Prabakaran et al., 2005)

Over the years, various methods have been developed to synthesize HA from synthetically obtained precursors. These methods vary in terms of the precursors used, processing cost, the morphology of the HA powder produced, Ca/P molar ratio as well as the particles size produced (Sadat-Shojai et al., 2013). The stoichiometric HA derived from these methods lacks the presence of trace amounts of ions in its lattice structure. These ions are shown in Table 1.2. Bone itself is regarded as a non-stoichiometric HA due to the presence of minor amount of ions in its HA lattice (Siddharthan et al.,2009). The presence of a minute quantity of these ions has been known to be beneficial to the bone as well as calcium phosphate based implants (Pietak et al., 2007). For an instance, magnesium ions play a role in bone mineralization. A decrease in its ionic content results in a decrease in osteoblast cell

activity, which translates to fragile bones. On the other hand, the presence of strontium ions is known for its capability in the formation of bone as well as the ability to suppress the resorption of bone. Besides that, sodium ions are beneficial in terms of bone metabolism (Siddharthan et al.2009), whereas the presence of silicon ions plays a significant role in bone formation as well as calcification (Pietak et al.,2007).

Table 1.2: Foreign ions in the HA lattice of human bone.

Cations		Anions	
Barium	Ba^{2+}	Carbonate	$CO2_3^{2-}$
Calcium	Ca^{2+}	Chloride	Cr^-
Iron	Fe^{2+} Fe^{3+}	Fluoride	F^-
Magnesium	Mg^{2+}	Phosphate	PO_4^{3-}
Potassium	K^+	Hydroxyl	OH^-
Silicon	Si^{4+}		
Sodium	Na^+		
Strontium	Sr^{2+}		

HA derived from natural resources and bin wastes are non-stoichiometric due to the various ionic substitution on its crystal structure for the OH^-, PO_4^{2-} and Ca^{2+} groups, making its usage in the development of bone like implants highly desirable (Best et al.,2008, Milovae et al.,2014). Synthetically derived HA (sHA) on the other hand requires various additional processes to incorporate these ions into its lattice structure which potentially increases the cost of production on top of its high cost in procuring these precursors (Landi et al.,2003; Li et al.,2007; Pietak et ak.,2007).

These drawbacks justify the usage of natural resources and bio waste as precursors in the synthesis of HA, as it is both sustainable and cost effective. Another inherent advantage in the usage of natural resources as precursor for HA is seen in the development of scaffolds. Interconnected porous networks are required in the development of scaffolds, as it plays a

significant role in the transport of metabolic waste, nutrients as well as cell attachment (Milovac et al., 2014: Tang et al., 2013). Polymer sponge replication (Ramay & Zhang, 2003; Tripathis & Basu, 2012), gel casting (Kim et al., 2011; Ramay & Zhang., 2003) and freeze casting (Deville et al., 2006; Tang et al., 2013) are some of the methods in which scaffolds are developed from synthetically-derived HA. These methods require various processing routes and conditions, making at a tedious development process. Indeed, a simple hydrothermal conversion of natural aragonite from cuttlefish bone at 200°C seen to result in a highly interconnected porous structure (Milovae et al., 2014). This further justifies the advantage of naturally derived HA.

1.3 RESEARCH OBJECTIVES

The current research aims at synthesizing phase pure hydroxyapatite based on the wet chemical precipitation method using eggshells as a calcium precursor. Sintering studies via conventional sintering is conducted on compacted as synthesized eggshells derived hydroxyapatite powder to evaluate its mechanical properties as well as its physical characteristics. In addition, different type of sintering additives with the oven sintering to compare the mechanical properties of hydroxyapatite. Hence the objective of the current research are shown below:

1. To synthesize high purity hydroxyapatite via a wet chemical precipitation technique using calcined waste eggshells as a calcium precursor and with additional of different sintering additives to obtain dense hydroxyapatite

2. To thoroughly investigate and evaluate the mechanical properties and physical characteristics of obtained hydroxyapatite.

1.4 SCOPE OF THE RESEARCH

The initial phase of the research was to prepare pure hydroxyapatite powder using novel wet chemical precipitation method via conventional drying. Different temperature from 700°C until 1000°C were carried out to determine the ideal of temperature where $CaCO_3$ in eggshells decompose to CaO. Wet chemical method was used to prepare the hydroxyapatite from the ideal temperature to produce complete CaO. The mechanical of the hydroxyapatite hence further to investigate via adding different additive sintering chemical (zinc oxide, aluminum oxide, magnesium oxide and titanium oxide). The Sintering hydroxyapatite hence compress into pallet and further sintering from 1050 until 1350°C. The effects of sintering temperature and the influence of sintering chemical as dopants on the hardness, density and microstructure of the sintered HA were evaluated.

1.5 THESIS OUTLINE

Chapter 2 provides a brief description on hydroxyapatite (HA) and biological apatite along with the various synthesis methods to produce HA. Besides that, this chapter also includes a detailed review on the various biogenic resources used to synthesize HA. In additional, a section is also allocated to the mechanical property evaluation of HA derived from biogenic resources.

In chapter 3, calcination of eggshells to produces CaO and various other processes in the synthesis of eggshell derived Hydroxyapatite (EHA) are discussed. Apart from that, the various experimental procedures to evaluate the mechanical properties and physical characteristics of as-synthesizes and sintered EHA are included in this chapter.

The results obtained from the study and the dimension sections are presented in Chapter 4. The results and discusses the physical characteristics of as-synthesized EHA powder and the CaO obtained from eggshells in terms of XRD, FTIR, EDS and powder morphology analysis. The second section analyzes the physical and mechanical properties of EHA based in a conventional sintering approach in relation to its physical and mechanical properties.

CHAPTER 2 LITERATURE REVIEW

2.1 INTRODUCTION TO HYDROXYAPATITE (HA)

Hydroxyapatite (HA), $Ca_{10}(PO_4)_6(OH)_2$, is a biomaterial which has a chemical structure similar to the mineral composition of human and mammalian bone. It is rendered as one of the few materials that are considered to be bioactive (Jayaswal et al.,2010) The image elements of HA are calcium and phosphorus with a stoichiometric Ca/P molar ratio of 1.667, where this ratio provides as indication of the phase composition (Kehoe, 2008). Ca/P molar ratios below 1.667 indicate in the formation of α and β tricalcium phosphate (TCP), $Ca_3(PO_4)_2$ upon synthesis. This is undesirable as the biodegradable characteristics of TCP are detrimental to the mechanical properties of HA. On the other hand, a Ca/P molar ratio higher than 1.667 results in the formation of calcium oxide (CaO) along with as-synthesized HA (Best et al.,2008).

The most intriguing characteristics of HA is its ability to rapidly integrate with the human body, particularly its indistinguishable union with the human hard tissue (Jayaswal et al., 2010). Nevertheless, the usage of HA is only limited to non-load bearing applications. This is ascribed to its poor mechanical properties, mainly its low fracture toughness (K_{IC}), of <1 MPa $m^{1/2}$ as compared to that of the human cortical bone within 2-12 MPa $m^{1/2}$ (Hench, 1991; Ramesh et al., 2008). The theoretical density of HA is 3.156gcm^{-3}. Achieving the aforementioned density requires consolidation of HA particles, which is commonly attained at elevated temperatures (Jayaswal et al., 2010; Kehoe,2008). However, decomposition of HA to its secondary phases was observed at higher temperature (Jayaswal et al.,2010). Therefore, synthesis of thermally stable HA is of paramount importance in attaining high relative density HA prior to decomposition. Till date, there have been several application of

HA, notably in the coating of metallic implants, scaffold formation, usage as bone fillers and bone cements (Best et., 2008)

2.2 BIOLOGICAL APATITE

Natural bone consists of organic as well as inorganic material. The organic constituents primarily comprise of collagen, whereas the inorganic materials on the others hand predominantly contain calcium and phosphate (Kehoe, 2008). Hydroxyapatite (HA) is regarded as the key mineral found in the bone structure, dentin and teeth. However, biological apatite commonly found in bones is generally carbonated apatite. Not only does the carbonate apatite exhibit a hexagonal crystal structure inherent to HA, it also generates XRD patterns that are analogous to HA (Kehoe, 2008). In terms of elemental analysis, the Ca/P molar ratio of biological apatite generally deviates from the stoichiometric HA ratio of 1.67. This is ascribed to the numerous ionic substitutions in the biological apatite crystal structures (Dorazhkin,2009).

Human bones are generally comprised of a dense outer layer called the cortical or compact bone and a mesh like internal layer known as the cancellous or trabecular bone (Dorozhkinm,2009). For terms of mechanical properties, differences between cortical and cancellous bones are rather apparent. This can be seen in Table 2.1 which compiles the mechanical properties of the human bone in terms of its elasticity modulus, fracture toughness and Vickers hardness. Porosity, solid matrix organization and mineralization levels affect the mechanical properties of cortical bone. However, this is not the case in cancellous bone (Kehoe, 2008: Orlovskii et al.,2002). Mineralized collagen fibrils are regarded as the building blocks of bone where a higher mineral to collagen ratio generally translates to stronger, but brittle bones. Cortical bones area generally superior compared to

cancellous bones in terms of mechanical properties, particularly its high strength and fracture toughness (Dorozhkin, 2009). This is attributed to the layered microstructure of the HA matrix in the cortical bone (Orlovskii etal.,2002)

Table 2.1: Mechanical properties of human cortical and cancellous bone. (Burcau et al.,2006: Hench, 1991: Kehoe, 2008; Orlovskii et al., 2002; Rho et al 1997)

Properties	Cortical Bone	Cancellous Bone
Density ($g\ cm^{-3}$)	1.6-2.10	0.03-0.12
Hardness (GPa)	0.30-0.60	~0.47
Young's Modulus (GPa)	3.90-25.00	0.04-1.00
Fracture Toughness (MPa $m^{1/2}$)	2.00-12.00	-

2.3 INTRODUCTION TO HA SYNTHESIS ROUTES

Over the years, a vast array of preparation methods have been developed to synthesize HA, where these methods vary from the wet chemical precipitation route (Mostafa, 2005: Ramesh et al., 2013), hydrothermal method (Zhang et al.,2009; Zhu et al.,2008), sol-gel route (Feng et al.,2005; Padmanabhan et al.,2009) and the mechanochemical method (Kim et al., 2000; Rhee 2002) However, only a handful of these methods are acceptable in terms of its capability and operational cost. This is due to the complicated and costly nature of certain processes, the requirement of diverse precursors, issues due to aggregation and agglomeration, as well as the wide variation in terms of particles size distribution (Sadat-Shojai etal.,2013). In this section, the characteristics of a few significant and commonly used HA synthesis routes are briefly discussed.

The wet chemical precipitation (WCP) route as shown in Figure 2.2, is regarded as the most preferred technique in the synthesis of HA where this is attributed to its simplicity in terms of usage as well as the requirement of inexpensive equipment (Nayak, 2010; Sadat-Shojai et al.,2013). This method is based on the titration process where either one of the precursors are added drop-wise to the other under continuous and non-vigorous stirring, in addition to maintaining the pH of the solution at a level above 10 (Padmanabhan et al.,2014; Ramesh et al.,2012; Sadat-Shojai et al.,2013; Yang 2005). The latter is achieved via the addition of either urea, ammonium hydroxide (NH_4OH), or sodium hydroxide (NaOH). Upon synthesis, the produced HA suspension is either aged or immediately washed, filtered, dried, crushed and sieved to obtain HA powder. The aging of HA varies from 3 hours (Rhee& Tanaka, 2000) up to 24 hours (Li, 2009). These variations have shown to affect powder morphology, particle size distribution and crystallinity as reported in the study conducted by Paz et al. (2012). In term of powder morphology, the WCP route generally produced rod-like (Catros et al., 2010; Okada & Furuzono, 2006) and needle like morphologies (Wang et al.,2010; Zhang et al.,2009) among other morphologies.

Synthesis of HA via the hydrothermal route is somewhat similar to the WCP route where the precursors are reacted to produce a HA suspension. However, the aging of the produced HA suspension is conducted at elevated temperature in a pressurized vessel or an autoclave. These conditions require relatively expensive equipment, thus increasing the overall cost to synthesize HA. Nonetheless, it has been shown that an increase in the hydrothermal temperature improves both phase stability as well as Ca/P molar ratio of the produced HA suspension (Sadat-Shojai et al.,2013). The elevated temperature varies from 80-300°C for durations up to 24 hours (Sadat Shojai etal.,2013). A significant disadvantage of this

method lies in its inefficiency in controlling powder morphology and particle size distribution. Nevertheless, manipulation of the hydrothermal temperature, heating duration and pH value of the HA suspension has shown to result in the growth of particles from a spherical morphology to short nano-rods (Sadat-Shojai et al.,2013)

Synthesis of HA via the mechanochemical method as shown in Figure 2.3, is regarded as a dry fabrication process which incorporates milling where solvents such as that employed in the WCP route are not used. The type and dimension of the milling ball used, the powder to ball mass ration and the rotational speed are some of the variables which can affect this synthesis route. In general, HA powder synthesized via the mechanochemical method was a well-defined structure (Sadat-Shojai et l.,2013). The integration of an aqueous phase in the mechanochemical method results in the formation of the wet mechanochemical route. The particular route is capable of generating localized elevated temperatures up to 700°C in the reaction while maintaining an overall temperature close to the room temperature. Thus, the wet mechanochemical method does not require an external heating source or a pressure vessel to successfully synthesize HA (Sadat-Shojai et al.,2013).

The sol gel synthesis method is advantageous as the molecular level mixing inherent to the process results in the formation of powder with improved chemical homogeneity, besides having a stoichiometric structure, large surface area and small particle sizes. This process begins with the reaction of the precursors in an organic or aqueous phase, followed by aging, gelation of the suspension, drying on a hot plate and calcination, which eliminates the presence of organic matter found in the gel-like substances (Sadat-Shojai et al.,2013). The process is schematically described in Figure 2.1. Prolonged aging is required as the reaction between the precursors to form the apatitic phase occurs at a slow rate, where an

inadequate aging duration leads to the formation of secondary phases (Sadat-Shojai er al., 2013). However, lengthy aging periods has shown to contribute to the growth and agglomeration of the HA particles (Feng et al.,2005). Besides the discussed synthesis method, other methods such as the solid state method, hydrolysis method, pyrolysis method, combustion method, sonochemical method and emulsion method have also shown to successfully produce HA (Sadat-Shojai et al.,2013)
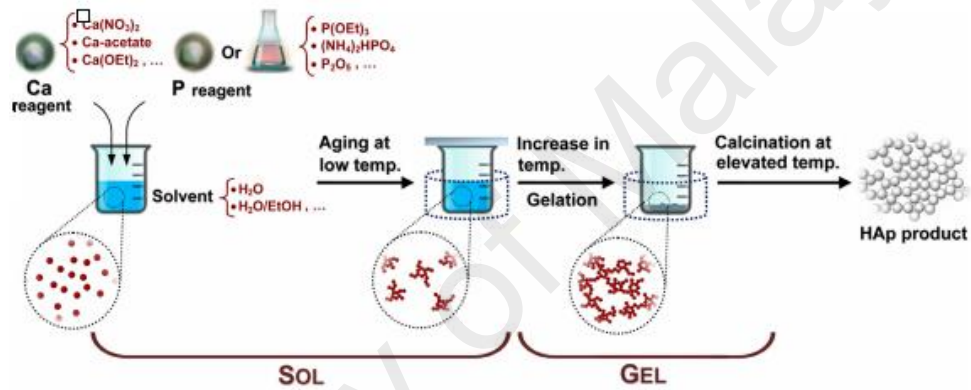
Figure 2.1: The synthesis process of HA via the sol gel route. (Sadat-Shojai., 2013)

Figure 2.2: The synthesis process of HA via the wet chemical precipitation(WCP) route (Sadat-Shojai et al.,2013)
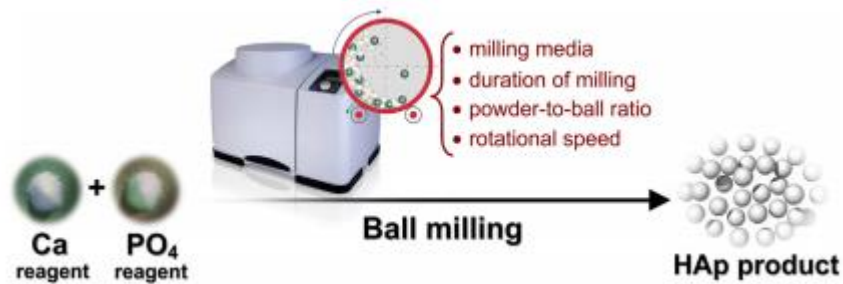
Figure 2.3: The synthesis process of HA via the mechanochemical method. (Sadat-Shojai et al.,2013)

2.4 SYNTHESIS OF HA FROM BIOLOGICAL RESOURCES

2.4.1 Synthesis of HA from eggshells

A staggering 4,351,667 tons of eggs were reported produced annually in a particular year in Mexico (Rivera et al., 1999), where in a different year, an annual statistic in India reported the production of an estimated 1,732,500 tons of eggs (Sasikumar & Vijayaraghvan , 2006). Out of this, 11 wt% of the total with is from the shell (Singh & Mehta, 2012), which will eventually be discarded as waste. This causes further environmental concerns. Eggshells are mainly composed of calcium carbonate ($CaCO_3$) which constitutes approximately 94 wt% of its total weight. The remaining 6 wt% is distributed between the organic matter present in the eggshell (4 wt%), Magnesium carbonate (1 wt%) as well as calcium phosphate (1 wt%). The high content of $CaCO_3$ contained in eggshells, as well as the presence of trace amount of ions such as Na^+, Sr^{2+} and Mg^{2+} makes it an attractive waste material to be used as a calcium precursor in the synthesis of HA (Ho et al.,2013; Prabakaran et al., 2005)

The first report usage of HA synthesized from eggshell was by Rivera et al. (1999), where waste eggshells were converted to calcium oxide (CaO) via a two stage heating process. The eggshells were first heated to 450C to remove various organic components, followed by heating at 900°C, initiating the decomposition of $CaCO_3$ to CaO. A hydrothermal route was employed to synthesize HA using the produced CaO and tricalcium phosphate ($Ca_3(PO_4)_2$) as the calcium and phosphorous precursor respectively. This was conducted in a sealed container at 1050°C for 3 hours using a ramp rate of 10°C/min. However, XRD analysis indicted the present of CaO and calcium hydroxide ($Ca(OH)_2$) alongside HA. This could be attributed to the incomplete transformation of $CaCO_3$, due to either a low annealing temperature or an insufficient heating duration. Over the years, the synthesis method pioneered by Rivera et al (1999), has been improved to obtain phase pure HA. In addition, various other synthesis methods have been developed using eggshells as a calcium precursor.

Synthesis of eggshell derived hydroxyapatite (EHA) has been achieved via a number of different synthesis routes such as, the wet chemical precipitation method (Dahlan et al., 2012; Hui et al., 2010; Ibrahim et al., 2013), hydrothermal method (Elizondo-Villarreal et al.,2012; Prabakaan & Rajeswari, 2009; Wu et al., 2013) wet mechanochemical method (Bardhan et al.,2011; Gergely et al., 2010), as well as the microware irradiation method (Krishna et al., 2007: Siddanrthan et al.,2009). Besides the various synthesis methods, different forms of calcium and phosphorus precursors have been employed to synthesis EHA. These different precursors are summarized in Table 2.2. Although a number of different calcium compounds have been used as calcium precursors, these precursors are ultimately derived from eggshells. Some of the commonly used chemical reactions adopted

in the synthesis of EHA area shown in equation (2.1) to (2.7). The $CaCO_3$ present in eggshells can be used as a calcium precursor in its carbonate state itself, or it can be converted to CaO via calcination,

The various calcination temperatures are also shown in Table 2.2. Calcination temperatures for eggshells range from 700°C to 1000°C. Elizondo- Villarreal et al. (2012) managed to calcine eggshells at 700C where XRD results indicated a complete conversion of $CaCO_3$ to CaO. Lee and Oh (2003), are one of the many researchers that have produced CaO by calcining eggshells at 900C, whereas Sopyan et al, (2011). On the other hand, carried out calcination at 1000°C to produce CaO. Dasgupta et al. (2004) carried out a study on various calcination temperatures within a range of 400°C to 1000°C. TGA/DTA results from that study showed that the minimal weight loss below 450°C is due to the oxidation of the organic compounds, as well as the absorbed water present in the eggshells structure. A significantly larger weight loss with as approximate value of 40 wt% was observed between 750°C to 900°C indicating that almost all of the $CaCO_3$ decomposed to CaO with a peak at 850°C. The remaining minute quantity of unreacted $CaCO_3$ is converted to CaO above 900°C.

These results are supported by the research conducted by Krishna et al. (2007) which reported an approximate weight loss 45 wt% between 50°C to 830°C based on TGA/DTA plot, indicating the peak calcination temperature. Similar results were obtained from the study conducted by Ho et al. (2013) where a weight loss of approximately 40 wt% was observed up to a temperature of 810°C with an endothermic peak in the DTA plot at 834°C. The peak temperature observed on the DTA plot indicates the phase transformation of $CaCO_3$ to CaO. Research has shown that the phase transformation of $CaCO_3$ occurs within

830°C to 850°C (Dasgupta et al., 2004; Ho et al., 2013; Krishna et al., 2007). However, the study conducted by Elizondo-Villarreal et al. (2012) indicates that CaO can be successfully produced via calcination at 700°C. A possible explanation for this phenomenon could be due to the longer holding time of 5 hours employed by the authors as compared to the norm of 1 to 3 hours.

Produced CaO has been known to be converted to calcium hydroxide $Ca(OH)_2$ (Dahlan et al.,2012; Hui et al.,2010) and calcium nitrate $(Ca(NO_3)_2$ (Ahmed & Ahsan, 2008; Dasgupta et al.,2004). However, $Ca(NO_3)_2$ is commonly formed by using $CaCO_3$ from eggshells along with nitric acid (HNO_3) (Bardhan et al., 2011; Ibrahim et ak.,2013; Siddharthan et al.,2009) other calcium precursors originating from eggshells have also been formed. Wu et al. (2013) produced $CaCl_2$ by reacting eggshell powder with hydrochloric acid (HCL) whereas Kumar et al. (2012) reacted crushed eggshells with Ethylenediaminetetraaccetic (EDTA) to produce a Ca-EDTA complex. Put of all the available calcium precursors, the most commonly used calcium precursor derived from eggshells are $Ca(OH)_2$ and CaO. On the other hand, the most common calcination temperature employed was at 900°C, even though $CaCO_2$ has been shown to decompose to CaO between 830°C to 850°C. A possible reason for this is to ensure that all the $CaCo_3$ is decomposed to CaO

Table 2.2: Synthesis description and characteristic of HA powder using eggshells as a calcium precursor.

No	Synthesis Method	Calcium (Ca) Precursor	Phosphorus (P) Precursor	Calcination Temperature (°C) Duration (hours)	Powder Morphology	Particle Size (nm)	Reference
1	WCP	CaO	K_3HPO_4	900	Circular	~41	Chaudhuri et al (2013)
2	WCP	$Ca(OH)_2$	H_3PO_4	900	Irregular	5000	Goloshehapov et al (2013)

3	WC+M	CaCl$_2$+ Fruit Extract	H$_3$PO$_4$	-	Needle Like /Rice lieke	<100	Wu et al (2013)
4	WCP	Ca(OH)$_2$	(NH$_4$)$_2$HPO$_4$	1000	Bar-like	L:300	Dahlan et al (2012)
5	WC+M	CaCO$_3$+EDTA	Na$_2$HPO$_4$	-	Flower like	L:500 to 1000 W: 100 to 200	Kumar and Girija (2013) Kumar et al (2012)
6	H	CaO	CaHPO$_4$	700	Micrometer sized whiskers	60	Eliondo-Villarreal et al (2012)
7	WM	CaCO$_3$	H$_3$PO$_4$	-	Irregular	~100	Gergely et al (2010)
8	WCP	Ca(OH)$_2$	Ca$_3$(PO$_4$)$_2$	900	Oval/Spherical	~400	Hui et al (2010)
9	WC+H	Ca(OH)$_2$	H$_3$PO$_4$+CTAB	900	Rod like	100 to 300	Prabaaran and Rajeswari (2009)

*synthesis Method acronyms: WCP = Wet Chemical Precipitation, WC= Wet Chemical, H+ Hydrothermal, WM= Mechanochemcial

*The calcination temperature is in reference to the decomposition process instead of the heat treatment process

*The letter (L) under the particles section represents length whereas the letter (W) represent width

$$10CaO+6K_2HPO_4+4H_2O\rightarrow Ca10(PO_4)6(OH)_2+12KOH \tag{2.1}$$

$$10CaO+6(NH_4)2HPO_4+4H_2O\rightarrow Ca10(PO_4)6(OH)_2+12NH_4OH \tag{2.2}$$

$$Ca(OH)_2+3Ca_3(PO_4)_2\rightarrow Ca_{10}(PO_4)_6(OH)_2 \tag{2.3}$$

$$10Ca(OH)_2+ 6(NH_4)_2HPO_4\rightarrow CA_{10}(PO_4)_6(OH)_2+12NH_3+18H_2 0 \tag{2.4}$$

$$10Ca(OH)_2+ 6H_3PO_4\rightarrow CA_{10}(PO_4)_6(OH)_2+18H_2 0 \tag{2.5}$$

$$10Ca(NO_3)_2+ 6H_3PO_4+2H_2O\rightarrow CA_{10}(PO_4)_6(OH)_2+20HNO_3 \tag{2.6}$$

$$10Ca(NO_3)_2+ 6(NH_4)_2HPO_4 +8 NH_4OH\rightarrow CA_{10}(PO_4)_6(OH)_2+20NH_4NO_3+6H_2 0 \tag{2.7}$$
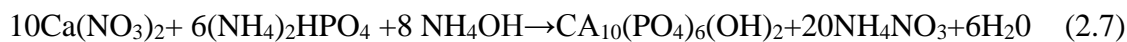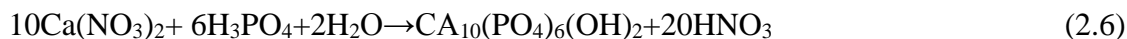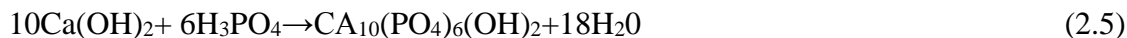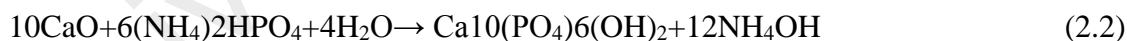
The biological HA found in the human bone structure are both nano-sized and resembles either rod like or plate like morphology with an approximately width of 5-20 nm and approximate length of 25-60 nm (Ferraz et al.,2004, Sadat-Shojai et al.,2013; Zhang et al.,2009, Zhou & Lee,2011). Hence, the synthesis if nano-sized HA powder long with the aforementioned powder morphologies is beneficial in term of its usage as bone replacement and implants as it is parallel to the physiological structure (Sadat-Shojai etal.,2013). In order for HA to be used effectively and efficiently in medical application, the synthesized powder should be morphologically well defined (Mostofa, 2005, Ramesh et al.,2013). This particular trait plays an important role in drug delivery applications where synthesized HA powder with a flower like morphology, as shown in Figure is postulated to be efficient in terms of drug loading and release (Kumar& Girija., 2013; Kumar et al.,2012)

Inherent properties of HA ceramic such as osteoconductivity, sinterability, mechanical properties, solubility, biocompatibility and bioactivity can be improved by controlling the morphology and particles size of the as-synthesized HA powder (Fathi et al,2009, Qiu et al.,2008; Zhou & Lee, 2011). Commonly faced issues such as micro-cracks in HA ceramic and other high temperature sintering related issues can be avoided by using nano-sized HA powder. This is due to the inherent characteristics of nano-sized HA which improved densification and sinterability (Sadat-Shojai et al.,2013)
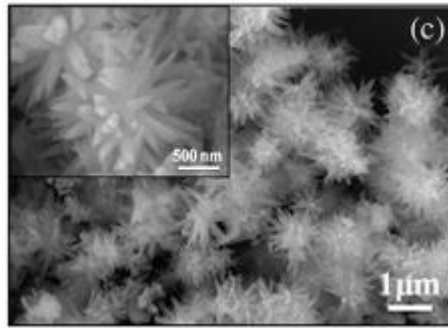
Figure 2.4: SEM image if the HA particle with a flower like morphology. (Kumar et al.,2012)

Nano size eggshells derived HA (EHA) with various powder morphologies have been successfully synthesized. HA particles with a spherical morphology are known to possess better properties as compared to powders with an irregular morphology. This can be beneficial in terms of achieving better coatings for hip implants (Luo & Nich, 1995). The detailed list of various particle sizes and powder morphologies is summarized in Table 2.2. The study conducted by Hui et al, (2010), successfully synthesized EHA powder with a spherical morphology and a particle size of -400nm. The authors employed a wet chemical precipitation method where $Ca(OH)_2$ and tri-calcium phosphate $(Ca_3(PO_4)_2)$ were used as calcium and phosphorus precursors respectively. Both precursors were mixed to form a suspension which was maintained at 90°C, followed by ageing for 24 hours to produce EHA.

Relatively fine nano-sized HA particles have been formed using eggshells as calcium precursors. This was observed in the research conducted by Sanosh et al. (2009) which was the only study to synthesize EHA via sol gel precipitation route, resulting in the formation of irregular shaped particles with an particles size of ~35nm. The sol gel precipitation route employed by the authors made use of $Ca(NO_3)_2$ and potassium dihydrogen phosphate

(KH_2PO_2) as the precursors. Synthesis of nano-sized EHA was achieved via the slow addition of KH_2PO_4 solution to the $Ca(NO_3)_2$ solution under rigorous stirring conditions at an optimum pH of 10 followed by overnight ageing. Besides that, Krishna et al. (2007) managed to synthesize EHA powder with a spherulic morphology and a particles size of 18nm using $Ca(OH)_2$ and diammonium hydrogen phosphate (($NH_4)_2HPO_4$). The study incorporated a combination of wet chemical synthesis and microware irradiation to synthesize the EHA powder. The produced $Ca(OH)_2$ and $(NH_4)_2(HPO)_4$ were mixed to form a solution before being irradiated in a microwave oven to produced HA powder. On the other hand, Ibrahim et al (2013) successfully synthesized EHA powder with an irregular morphology and a particle size of 8.9nm. The authors used $Ca(NO_3)_2$ and H_3PO_4 as the starting precursors to synthesize the EHA powder as compared to $Ca(OH)_2$ and $(NH_4)_2HPO_4$ used by Krishna et al. (2007)

The synthesis method incorporated by Ibrahim et al. (2013) played a significant role in the fine particle size of the EHA powder produced. Eggshells were initially dissolved in HNO_3 to produce $Ca(NO_3)_2$ under vigorous agitation followed by the addition of orthophosphoric acid (H_3PO_4) to the produce $Ca(NO_3)_2$ solution at the rate of 200ml/hour. The steady flow of H_3PO_4 into the $Ca(NO_3)_2$ solution maintained the pH of the mixture which translated to the dissolution, formation and maturation of the reactants at an effective rate, hence producing fine nanoparticles. In general, synthesis of HA via the wet chemical precipitation route has been known to produce larger particles, whereas the microware irradiation route on the other hand, produces fine particles (Smolen et al., 2012). However, the particle size of HA synthesized by Ibrahim et al. (2013) was smaller compared to the HA synthesized by Krishna et al. (2007). Indicating that synthesis is not the only factor that can influence the

particles size of the HA powder produced. Other factors such as the type of precursor used, as well as the aforementioned acid addition rate can significantly alter the size of the HA particle produced.

As mentioned previously, HA synthesized via the wet chemical precipitation method has been known to produce large particles with the exception for the EHA powder synthesized by Ibrahim et al. (2013) and Chaudhuri et al. (2013). The synthesis method adopted by Chaudhuri et al.(2013) different from the wet chemical precipitation method implemented by different researches in terms of the preparation method used $Ca(OH)_2$ was used as the calcium precursor where the CaO used to produce $Ca(OH)_2$ was obtained via calcination of eggshells at 900C for 3 hours, whereas di-potassium phosphate (K_2HPO_4) was used as the phosphorous precursor. The variation in the preparation method lies in the duration of the synthesis process. CaO was added to deionized water and K_2HPO_4 to form a solution which was left to self-react for different durations ranging from 1-7 days. The produced white precipitate was then filtered and dried in an oven at 37°C for 7 days, where this time consuming synthesis process ranged from 8 to 14 days. However, nano-sized HA particles were produced with an approximate of 41 nm with a circular morphology.

The self-reaction duration affected the agglomeration of the articles where a longer duration resulted in particles being closely compacted compared to the reaction with a lesser duration. The synthesis of HA derived from eggshells via the wet chemical precipitation route is the most common preparation method due to its simplicity and usage of inexpensive equipment. On the contrary, synthesis via the hydrothermal route us the least preferred route based on available literature. Probakaran and Rajeswari (2009) synthesized EHA using a combination of wet chemical precipitation and a hydrothermal route. EHA

particles with sizes ranging from 100-300 nm were produced with rod like morphologies similar to biological HA found in the human hard tissue. Figure 2.5 shows the growth process of HA particles with rod-like morphologies under hydrothermal conditions where this particular process occurs in two main stages which are the nucleation stage followed by the growth stage. During nucleation, the formation of crystalline nuclei is observed due to the reaction of precursor ions in the synthesis medium. This is followed by the growth stage where the particle morphs into its final shape and size which is controlled via conditions during the hydrothermal treatment (Sadat-Shojai et al.,2013)
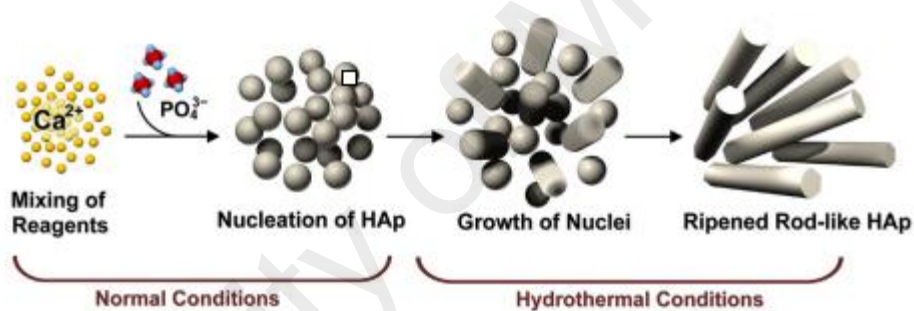
Figure 2.5: The growth process of HA particles under normal and hydrothermal conditions. (sadat-Shojai.,2013)

In a study conducted by Prabakaran and Rajeswari (2009), $Ca(OH)_2$ and H_3PO_4 were used as precursors and cetyltrimethyl bromide (CTAB) was added to the H_3PO_4 solution and left overnight. CTAB is a cationic surfactant which is commonly used to control particles morphology. However, the authors used it to control the crystallization of the produced HA. The H_3PO_4 and CTAB solution were added drop wise to the $Ca(OH)_2$ solution which was produced by adding calcined eggshell to distilled water. The produced solution was transferred to an autoclave followed by hydrothermal treatment at 160°C for 10 hours. The

treatment duration was shown to affect the size of the particles. A longer duration time produced uniform EHA particles whereas shorter treatment durations produced highly agglomerated particles. Besides the treatment duration the authors observed that the usage of CTAB helped ensure the synthesis of nano-sized HA particles under optimum conditions where the molar ratio of CTAB to PO_4^{2-} is 1:1.

The longer treatment duration as well as the expensive equipment required could possibly be a deterrent to the usage of the hydrothermal route in synthesizing HA. In addition, the incapability of the hydrothermal method to control the morphology of nanoparticles could also be a contributing factor to its limited usage in the synthesis of HA derived from eggshells (Sadat-Shojai et al 2013). Elizondo-Villarreal et al. (2012) also employed the hydrothermal method to synthesize HA however, the authors used CaO and calcium dibasic phosphate ($CaHPO_4$) as precursors. The precursors were added to a solution acidified by vinegar and placed in a Teflon vessel followed by hydrothermal heating at 170°C for 48 hours. After filtration and drying, EHA powder with nanometer sized whiskers with an average particles size of 60nm was produced. The smaller particles size of the EHA powder produced by the method proposed by Elizondo-Villarreal et al. (2012) as compared to the synthesis method proposed by Prabakaran and Rajeswari (2009) could be due to the longer heat treatment duration of 48 compared to 10 hours. Besides that, the usage of different precursors could also be a contributing factor to the smaller particle size produced.

Krishna et al. (2007) synthesized EHA powder with fine nano sized HA particles using a combination of a wet chemical and microware irradiation method. A similar approach was implemented by Kumar et al. (2012) except that different calcium and phosphorous precursors were used and the synthesized dendritic like structure of the HA particles had a

length of 500-1000 nm and width of 100-200 nm. The larger particle size produced by Kumar et al. (2012) compared to Krishna et al. (2007) was due to the usage of EDTA in the calcium precursor. The usage of EDTA has been known to control particles morphology where nano-rods were grown radially from a central spherical core to form particles with a dendritic nanostructure, hence the formation of larger particles (Sadat-Shojai et al.2013). A graphical description of the usage of EDTA in manipulating particles morphology was shown in Figure 2.6. The synthesis method implemented by Kumar et al. (2012) made use of disodium phosphate (Na_2HPO_4) and Ca-EDTA complex as phosphorus and calcium precursors respectively. The Ca-EDTA complex was produced by adding crushed eggshell to a 0.1M EDTA solution. Na_2HPO_4 was added slowly to the Ca-EDTA solution to produce a mixture with a final pH of 13 before being subjected to microware irradiation for 10 minutes.
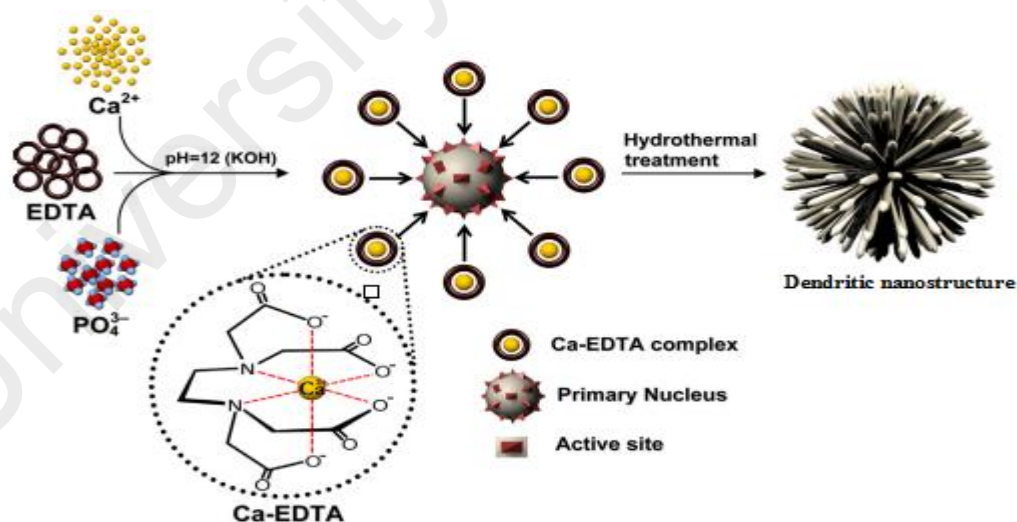
Figure 2.6: The influence of EDTA in the synthesis of HA particles with a flower like morphology via a hydrothermal route. (Sadat-Shojai et al.,2013)

In another work, Siddharthan et al (2009), Bardhan et al.(2011) and Dasgupta et al.(2004) synthesized HA using similar calcium and phosphate precursors Bardhan et al.(2011 and Dasgupta et al (2004) employed the wet chemical precipitation route whereas Siddharthan et al. (2009), synthesized HA using microwave irradiation $CA(NO_3)_2$ and $(NH_4)_2HPO_4$ were used as the calcium and phosphate precursors respectively. However, Siddharthan et al (2009) Bardhan et al (2011) reacted $CaCO_3$ with HNO_3 whereas Dasgupta et al. (2004) reacted CaO with HNO_3 to produced $Ca(NO_3)_2$. The synthesis is via microware irradiation produced platelet like particles with a length of 55-666 nm and a width of 12- 17 nm. On the other hand, the wet chemical precipitation led to relatively large particles having a size of 390 nm and 4770 nm respectively. The smaller particles size obtained by Bardhan et al.(2011) compared to Dasgupta et al. (2004) was due to the ball milling of the produced HA powder. Once again, the synthesis via the microware irradiation route produced fine nano-size particles. The usage of similar precursors rules out other factors that could potentially affect the size of the particles.

Another comparison can be seen in the researchers conducted by Krishna et al. (2007) and Dahlan et al. (2012) where similar precursors and different synthesis methods were used to produce EHA. $Ca(OH)_2$ and $(NH_4)_2HPO_4$ were used as the calcium and phosphorous precursors respectively. The wet chemical precipitation method used by Dahlan et al.(2012) produced bar-like particles with a length of 300 nm as compared to the HA particles with a spherulite morphology and a particles size of 18 nm synthesized by Krishna et al.(2007). This provides a further confirmation that the wet chemical precipitation route generally produces larger particles as compared to the microware irradiation method. The wet chemical precipitation route employed by Goloshehapov et al.(2013) produced HA powder

with by far the largest particles size of 5 μm. The authors mixed calcined CaO to distilled water to produce $Ca(OH)_2$ followed by titration using H_3PO_4 to produce EHA powder with an irregular morphology.

Biological apatites have a low crystallinity as well as small dimension and these inherent characteristics are to be incorporated in the synthesis of HA (Dorozkikin, 2009). Synthesis of HA with a low crystallinity has shown to increase solubility as well as osteoblast cell adhesion (Balasundaram et al., 2006; Valet-Regi, 2001, Xue et al., 2004). Also, a study conducted on plasma sprayed. HA coating onto Ti-6A-4V rods by Xue et al. (2004) indicated that HA with a low crystallinity plays an important role in the initial fixation of the bone. However, HA coating with a high crystallinity exhibited a higher shear strength between implant and bone in top of being a more suitable candidate for long term implantation.

EHA powder with a platelet like morphology with both low and high crystallinity has been synthesized via a rather uncommon synthesis method by Ahmed and Ahsan (2008). The authors implemented a wet chemical precipitation route both Cao and $CaCO_3$ to produce $Ca(NO_3)$, here after used as the calcium precursor and $Na_2HPO_4.12H_2O$ as a the phosphorous precursor. EHA powder with a platelet like morphology was also synthesized by Siddharthan et al. (2009) using similar calcium and phosphorus precursors. However, Siddharthan et al. (2009) employed a microwave irradiation route whereas Ahmed and Ahsan (2008) made use of a wet chemical precipitation route.

Two different synthesis routes were observed in the study done by Ahmed and Ahsan (2008), where the first synthesis route was based on the usage of CaO to produce $Ca(NO_3)_2$ whereas the second route made use of $CaCO_3$ to produce $Ca(NO_3)_2$. After completing the

wet chemical precipitation procedure, the filtered and dried precipitate produced via the first route was crushed to produced fine EHA powder, whereas the precipitate from the second route was calcined at 900°C for 30 minutes to produce EHA powder XRD results indicated that the EHA produced via the first route had a low crystallinity, whereas the second route exhibited a high crystallinity. This shows that usage of an unconventional wet chemical precipitation method using different calcium precursors derived from eggshells is capable of producing HA powder with both a low crystallinity as well as one with a high crystallinity.

The usage of cationic surfactants such as CTAB as well as chelating agents such as EDTA (Kumar et al., 2012; Prabakaran & Rajeswari. 2009) has been known to be able to manipulate powder morphology. However, an interesting synthesis approach by Wu et al. (2013) led to the formation of EHA with needle-like and rod like powder morphologies by incorporating fruit extract solutions into the calcium precursors solutions instead of commonly used chelating agent and cationic surfactant. The synthesis method incorporated by Wu et al. (2013) was similar to the one employed by Prabakaran and Rajeswari (2009) where a combination of a hydrothermal and a wet chemical route was used. In this study, Wu et al. (2013) used calcium chloride ($CaCl_2$) as the calcium precursor which was produced by reacting crushed eggshells with HCL whereas H_3PO_4 was used as the phosphorus precursor.

In a study reported by Prabakaran and Rajeswari (2009), CTAB was added to the phosphorus precursor, whereas Wu et al, (2013) added the fruits extract solutions to the $CaCl_2$ solution instead. Grape, sweet potato and pomelo peels were used as the fruit waste. Initially, 80 grams of the fruits waste was boiled in 1000 ml of water followed by filtration

where 5 ml of the filtrate and added to 20 ml of the calcium precursor solution containing $CaCO_3$ and HCL. The H_3PO_4 was then added slowly to the calcium and fruits extract solution while the pH was maintained at 10 using ammonium hydroxide (NH_4OH). The produced mixture was then hydrothermally reacted at 150°C in a Teflon-lined steel autoclave for a reaction time of 24 and 72 hours to produce EHA powder. Particles with an approximate size of less than 100 nm were synthesized by Wu et al,(2013) as compared to the EHA powder synthesized by Prabakaran and Rajeswari (2009) that had a wider particles size range of 10-300 nm. The larger HA particles size derived by Prabakaran and Rajeswari (2009) was due to the shorter reaction time of 10 hours as compared to Wu et al.(2013) who employed a reaction time of 24 and 72 hours. The morphology of the powder on the other hand transformed from a needle-like structure at a reaction time of 24 hours to a rod like morphology when the reaction time was prolonged to 72 hours. These morphologies are shown in Figure 2.7 and 2.8.

ICP-AES results indicated the presence of a trace amount of Na^+, Mg^{2+} and Sr^{2+} in the synthesized EHA powder containing the pomelo peel extract. The outcome of thin research suggests that a variation of hydrothermal reaction times as well as the usage of fruit waste extract, particularly the usage of pomelo peel has the capability of influencing particle size as well as particle morphology. It is postulated that the alterations of both particles size and morphology is due to the presence of limonene from the pomelo peel extract. Besides that, the presence of trace amounts of ions in the synthesized EHA can be beneficial in terms of biological performance in implant materials, due to its similarity with the biological apatite.
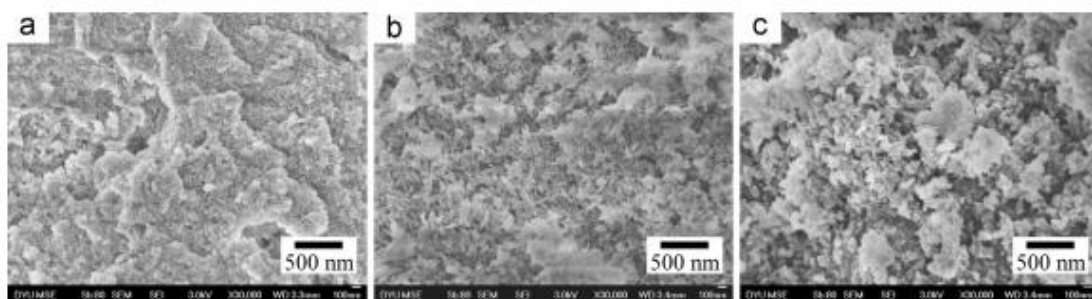
Figure 2.7: SEM images of HA synthesized via a hydrothermal route at 150°C for 24 hours using a mixture of fruits waste extract and CaCl$_2$ derived from eggshells. (a) Grape peel, (b) Sweet potato peel and (c) pomelo peel (Wu et al.,2013)
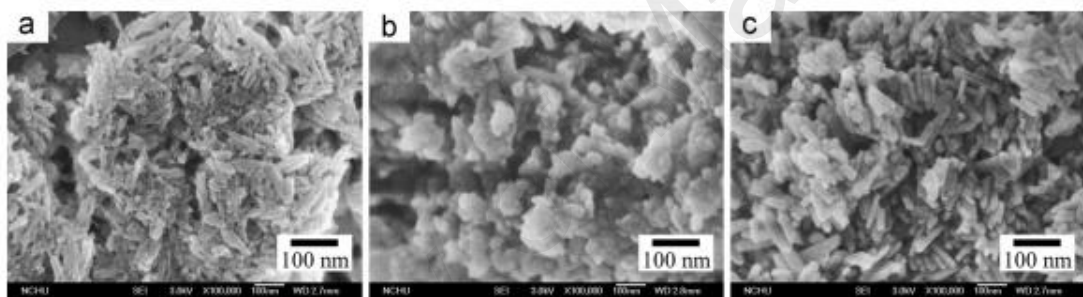
Figure 2.8: SEM images of HA synthesized via a hydrothermal route at 150°C for 72 hours using a mixture of fruit waste extract and CaCl$_2$ derived from eggshells. (a) Grape peel (b) sweet potato peel (c) Pomelo peel (Wu et al,2013)

The usage of CaCO$_3$ as calcium precursors from eggshells to synthesize HA on its own without the addition of EDTA has been employed by both Gergely et al. (2010) and Balazsi et al (2013). Both these authors adopted a wet mechanochemical route and H$_3$PO$_4$ was used as the phosphorus precursor. Gergely et al.(2010) synthesized EHA using an attrition mill as well as a ball mill. A 50:50 wt% ratio of eggshell powder to H$_3$PO$_4$ was milled in an attrition mill 5 hours at 4000 rpm and in a ball mill for 10 hours at 350 rpm. SEM scans revealed the synthesis of EHA powders with an irregular morphology using the ball mill whereas the attrition mill produced EHA powder with a globular morphology. Finer

particles with an approximate size of 100 nm were produced using the attrition mill as compared to the ball mill.

2.5 Sintering Additives

Besides the parameter like pH, sintering temperature and sintering time, adding sintering additives (also known as dopants) was reported to be cost effective and have beneficial effects on the sinterability of HA (Suchanek et al., 1997; Oktar et al., 2007; Ramesh et al., 2007b). The sintering additives should significantly enhance the densification without decomposition of HA, prohibit abnormal grain growth of HA grains and hence improve the toughness of HA ceramics. The decomposition of HA into secondary phase such as CaO is unfavorable as it would affect the biological performance of HA. Hence, various studies have been carried out to study the effects of different sintering additives on the phase stability of HA especially upon sintering. Suchanek et al. (1997) have doped HA with 5 wt% of selected sintering additives such as K_2O, Na_2O, MgO, Al_2O_3, SO_2, Li_2O, KCL and S^-. All the doped HA samples were subsequently sintered at $1000°C - 1100°C$. Exaggerated grain growth was not observed in the samples studied. The addition of K2CO3, Na2CO3, KF and all sodium phosphates was found to improve the sinterability of HA. The authors further revealed that other than the undoped HA, KCL and β-NaCaPO4, all other additives investigated caused either decomposition of HA into β-TCP or formation of CaO throughout the sintering regime employed. These secondary phases should be avoided as it increases the biodegradability of the HA ceramics. The authors found that β-NaCaPO4 would be an effective sintering agent as it significantly enhances densification without affecting the HA phase stability.

It was found that the amount of the dopant addition has effects on the phase stability of HA. Tolouei et al. (2011) noticed that doping HA with 0.8 wt% or more resulted in the formation of secondary phases such as β-TCP when sintered at 1250°C and the percentage of β-TCP formation increased when the amount of nano-silica increased. The decomposition of HA into β-TCP was found to hinder the densification and mechanical properties of HA as the density and hardness achieved for doped-HA was lower than those of the pure HA. This is attributed to the differential shrinkage between HA and the secondary phases formed at the sintering temperature (Rao & Kannan. 1999). The findings correlate well with the findings carried out by Xu and Khor (2007) who reported that the apatite structure became less stable and a secondary phase of β-TCP was detected in all the samples doped with silica. Similarly, Kutty and Singh (2001) found that the HA phase decreases with increasing Y-TZP content in the system regardless of sintering temperature employed. The presence of α-TCP, β-TCP and CaO was detected, indicating that HA phase was disrupted by the addition of Y-TZP.

The addition of dopants not only affects the thermal stability of HA but also influences the mechanical properties of the ceramic. The influences of additives on the microstructure and sinterability of HA using 0.05 wt% to 1 wt% manganese oxide (MnO_2) has been studied by Ramesh et al. (2007b). According to Ramesh et al. (2007b), the doping of 0.05 wt% MnO_2 was proven to obtain a hardness of 7.58 GPa and fracture toughness of 1.65 MPam$^{1/2}$ as compared to 5.72 GPa and 1.22 MPam$^{1/2}$ for undoped HA. It was found that the hardness of HA was closely related to the grain size. From Table 2.2, it was seen that 0.05 wt% doped HA sample had the smallest grain size and hence highest hardness and fracture toughness.

Besides, the authors found that the addition of 1 wt% MnO_2 was found to be detrimental to hardness of the sample as the hardness marked the lowest value at 5.32 GPa.

Table2.3: Grain size at which maximum hardness were measured for undoped and MnO2-doped HA. (Ramesh *et al*., 2007b).

MnO_2 Content (wt%)	Grain Size (µm)	Maximum Vickers Hardness (GPa)
0 (undoped)	0.50	7.21
0.05	0.47	7.58
0.10	0.58	7.00
0.30	0.52	7.30
0.50	1.03	7.04
1.00	1.56	5.32

On the other hand, Oktar et al. (2007) did a study on the sinterability of HA when doped with a variety of dopants. In this experiment, with the objective of improving the sinterability and mechanical properties of HA, it was doped with 5 wt% and 10 wt% of SiO_2, MgO, Al_2O_3 and ZrO_2. The presences of these oxides in HA are encouraging as they can act as crack arresters which will directly reduce the brittleness of HA. From their work, doping HA with 5 wt% MgO gave the best sintering result because it leads to denser HA compared to other dopants while the addition of SiO_2 caused a collapse in the hardness and density of HA. The additions of Al_2O_3 and ZrO_2 did not exhibit significant improvement in mechanical strength of HA.

The beneficial effects of the addition of MgO was supported by Tan et al. (2013). As presented in Figure 3.16 (a), doping of pure HA with different amounts of MgO noticeably enhanced the fracture toughness with the highest value recorded at 1.48 $MPam^{1/2}$ for 1.0 wt% MgO-doped HA as compared to 1.08 ± 0.05 $MPam^{1/2}$ measured for the undoped HA when sintered at 1150°C. This value is encouraging as other researchers who doped HA

with different additives such as zirconia (Kim et al, 2003), alumina (Champion et al., 1996) and titania (Manjubala and Kumar, 2000) obtained fracture toughness ranging between 1.0-1.4 MPam$^{1/2}$. Moreover, there are reports indicating that decomposition would occur when HA is doped with these dopants. However, in their study, the phase stability of HA was not disrupted by the addition of MgO as pure HA phase remained for all the doped and undoped samples throughout the sintering regime. Furthermore, hardness and relative density have greatly increased in HA with the reinforcement of MgO in the HA matrix. With the addition of MgO, the hardness of HA as maintained in a high range of ~6 GPa to 7.52 GPa even at considerably low sintering temperatures as shown in Figure 2.9 (b).
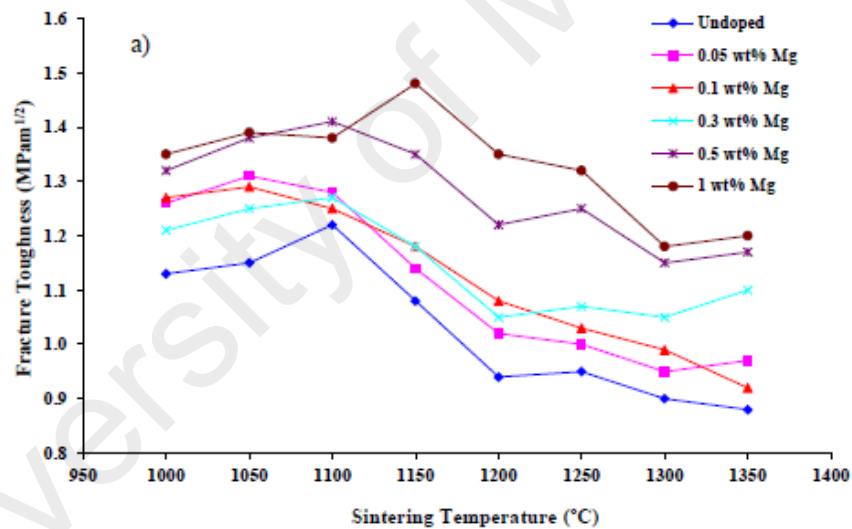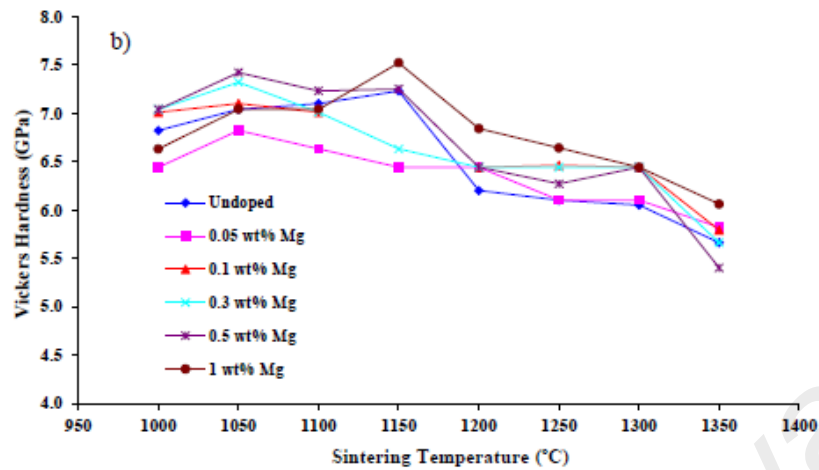
Figure 2.9 (a) and (b): Comparison of fracture toughness and Vickers hardness of different dosage of MgO-doped and undoped HA (Tan et al., 2013)

In summary, this chapter has provided an overview on the various methods employed to synthesis phase pure HA from biogenic and waste resources. Waste materials and natural resources such as eggshells are variety of sources and research proved have been successfully used in the synthesis of hydroxyapatite (HA). Hence, particular attention has to be paid to further improve the strength and other properties of HA by adding the sintering additive so that in can benefit human in future.

CHAPTER 3 METHODOLOGY

In this chapter, pertinent experiments, procedures and characterization methods related to the present research are discussed in detail.

3.1 Extraction of calcium precursor from eggshells

In this research, eggshells are used as a source of calcium for the synthesis of HA via the wet chemical precipitation route. A batch of 60 eggs was purchased from the local hypermarket. The remaining eggshells upon consumption were cleaned and air dried before the removal of the inner membrane layer. The membraned eggshells were then washed once again using distilled water followed by air drying. Cleaned and dried eggshells were then crushed to a fine powder consistency using a pestle and mortar. Figure 3.1 depicts the eggshells used in this study.
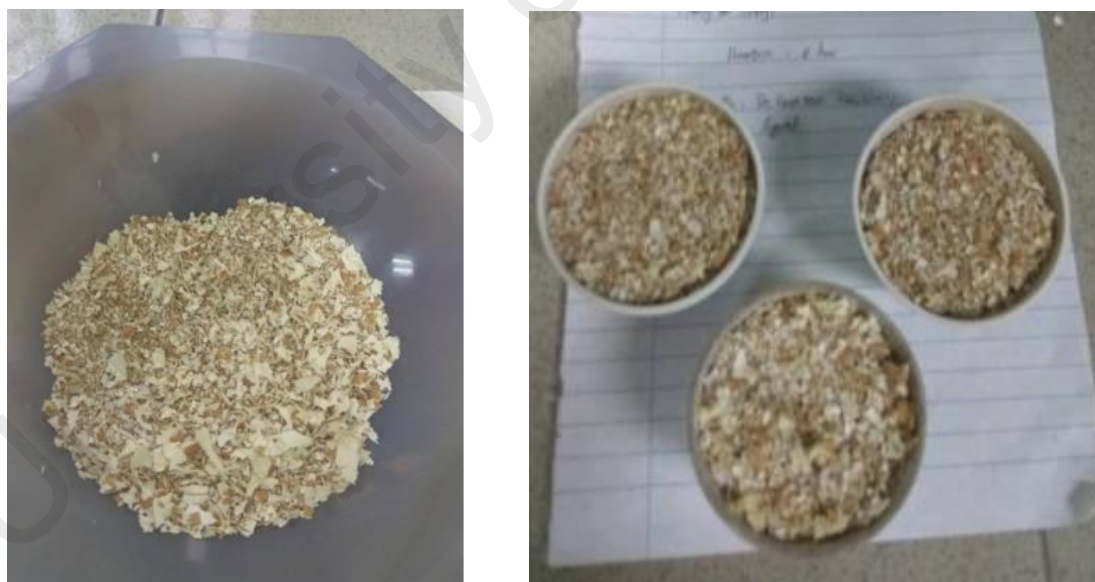
Figure 3.1: The eggshells that were used in the study: (a) Crushing processor eggshells using a pestle and mortar, (b) Finely crushed eggshells in small quantities placed in crucibles for calcination in a box furnace.

Conversion of $CaCO_3$ present in eggshells to CaO is achieved via calcination at elevated temperatures. The decomposition of $CaCO_3$ to CaO is shown in equation (3.1). Small quantities of finely crushed eggshells are placed in crucibles as shown in Figure 3.1 (b) before calcination in a box furnace (see Appendix A) The crushed eggshells are calcined at five different temperatures in order to determine the most suitable calcination temperature based on the purity of the CaO produced as well as its crystallinity. These temperatures are at 700,800, 850, 900 and 1000°C with a 10°C min^{-1} (heating and cooling) ramp rate and a holding time for 3hr.

$$CaCO_3 \rightarrow CaO + CO_2 \tag{3.1}$$

3.2 SYNTHESIS OF HYDROXYAPATITE (HA) POWDER

The synthesis of HA in the present study is based on the wet chemical precipitation route employed by a number of researcher (Goloshechapov et al., 2013: Prabakaran et al., 2005: Singh & Mehta, 2012) where CaO obtained via calcination of eggshells and H_3PO_4 (85% solution, Merck) were used as the starting precursors. The synthesis of HA is this study follows the chemical reaction shown in equation (3.2) The detailed synthesis of HA from eggshells (EHA) via the wet chemical precipitation route employed in this study is shown in the flowchart in Figure 3.2.

$$10Ca(OH)_2 + 6H_3PO_4 \rightarrow Ca_{10}(PO_4)_6(OH)_2 + 18H_2O \tag{3.2}$$
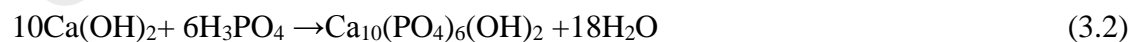
Appropriate amounts of calcined eggshell (CaO) were first weighed and added to distilled water to produce $Ca(OH)_2$. The produced $Ca(OH)_2$ slurry was stirred for 15 minutes using a magnetic stirrer before ultrasonication in a water bath for 3 hours.

The produced $Ca(OH)_2$ slurry after ultrasonication was stirred using a magnetic stirrer for an additional 15 minutes to create a homogenous suspension.

Pre-determined amounts of H_3PO_4 (85% solution, Merck) was added to 100 ml of distilled water followed by stirring for approximately 15 minutes before the titration process.

The mole ratio of the CaO and H_3PO_4 employed in the present research was 1.67: 1 in order to synthesize phase pure HA. The titration process made use of H_3PO_4 and $Ca(OH)_2$ as the titrant and analyte. The H_3PO_4 solution was added dropwise to the $Ca(OH)_2$ suspension at a rate of 10-20 drops/ minutes for an approximate 2 hours under stirring conditions using a magnetic stirrer.

Throughout the titration process, the pH of the solution was maintained at a level greater than 1-.5. This was achieved via the addition of ammonia hydroxide (NH_4OH) (25%, Sigma-Aldrich). A total of 50ml of NH_4OH was added to the analyte when the pH level dropped towards the end of the titration process. Besides a drop in pH, an increase in the viscosity of the analyte can provide an indication for the addition of NH_4OH.

Upon completion of the titration process, the suspension was stirred for an additional 1 hour followed by ageing of the HA suspension for 24 hours to complete the chemical reaction described in equation (3.2)

After the 24-hour ageing period, the produced HA suspension was stirred for 15 minutes before filtration to break up sedimentation due to the settling of HA particles. The filtered precipitate was then rinsed with approximately 4000ml of distilled water to wash off residual ammonia present in the precipitate.

The filtered and cleaned precipitate was dried in an oven at 60°C for 24 hours followed by crushing of the dried filtered cake. The produced powder after crushing was then sieved using a test sieve with an aperture size of 212 μm to produce uniform sized HA particles.

Figure 3.2: Above diagram showed the procedure of the synthesis of HA via wet chemical precipitation route.

3.3 Adding of Sintering Additive Material

In a typical procedure, both powders (hydroxyapatite powder (HA) and additive powder) are measured according to the respective ratio (composition) and put into a beaker containing approximately 200 ml of ethanol. 0.5 wt % sintering additive powders (Magnesium oxide, zinc oxide, alumina and titanium oxide) are mixed with hydroxyapatite through a process involving ultrasonic and ball milling. Suspension was placed in an ultrasonic bath at 28–34 kHz for 22 minutes to improve dispersion of additive powder in the HA powder. Upon completion of the ultra-sonication, the mixture is poured into a high-density metal bottle (50 ml) with 3 mm diameter zirconia balls as the milling media. The mixture was ball-milled for 1 hour at rotating speed of 350 rpm. (Volume suspension 30ml with 4 zirconia ball)

During the ball milling process, the HDPE bottles was shaken every 15 minutes to ensure that the mixture mixed well. Immediately after the milling process, the slurry is separated from the milling media through a sieve and was dried overnight in an oven at 60°C. The dried filter cake is crushed and sieved to obtain ready to press additives doped HA powders. Throughout the powder preparation process, care is taken to avoid contamination of the slurry by foreign particles. The milling procedures are kept the same for all level of dopant to ensure a fair comparison of performance. All the pressed HA pellets are sintered in a conventional furnace at a temperature of $1050^{\circ}C$–$1350^{\circ}C$.

Figure 3.3. 4 type of additive added together with HA powder.
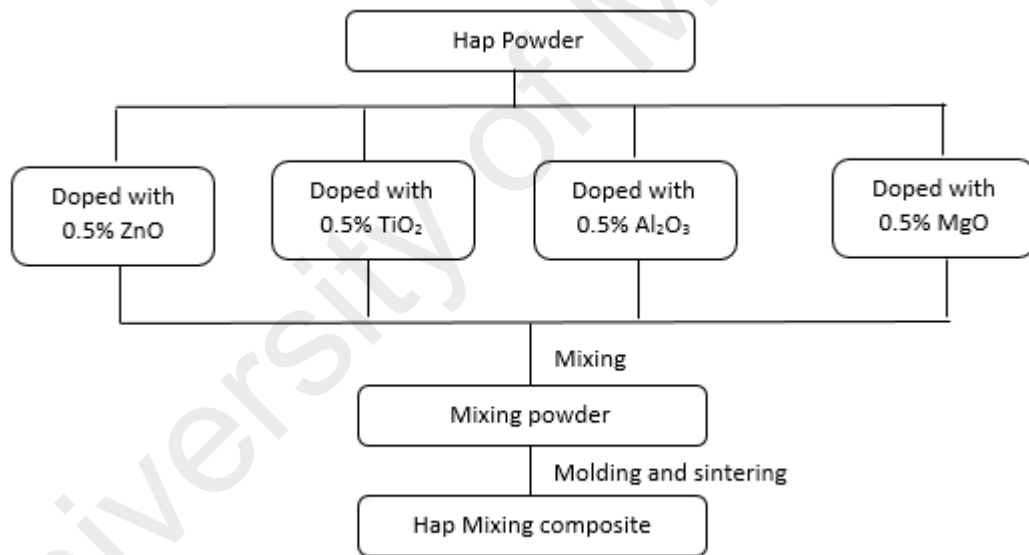
Figure 3.4. Flow chart showing the process for producing Mixing composite.

3.4 PREPARATION OF GREEN SAMPLES

Upon synthesis of the eggshell derived HA (EHA), the crushed and sieved powder was shaped into disc samples. The disc samples were formed to facilitate relative density measurement and the Vickers microhardness test as the aforementioned tests cannot be conducted ion powder samples. The disc (20mm dia. X 5 mm thickness) samples were prepared via uniaxial pressing (see Appendix) at a pressure of 5- 6 tonnes with a holding time of 1 minute before the removal of the sample from the die. The process of forming a disk sample is shown in Figure 3.5 where the lower punch was first attached to the die, followed by the addition of 1.5 grams of sieve of EHA powder into the die. Pressure was then applied to the upper punch as seen in Figure 3.5 (b). The die was then inverted pressure as shown in Figure 3.5 (d). From Chen and his colleagues study (2007), crack can be formed during the removal of the of the disc sample by subjecting the die set to an applied disc sample from the die due to die wall- particle friction. (Chen et., 2007).
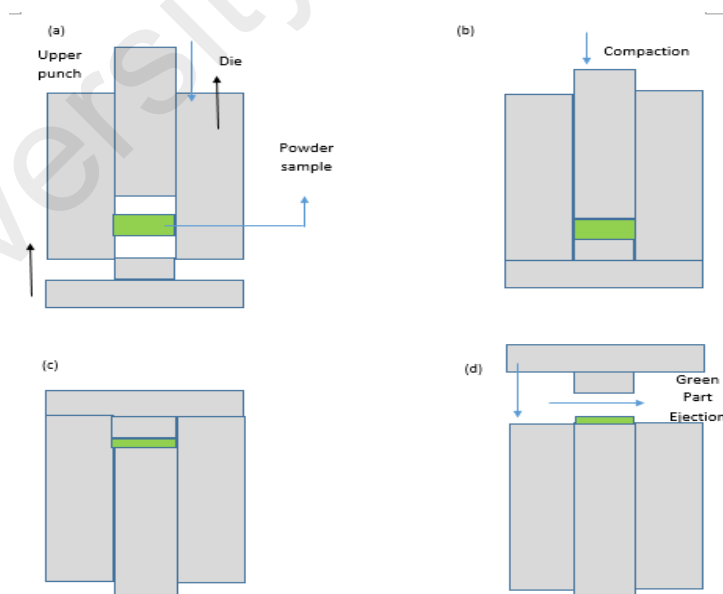
Figure 3.5. The above diagram show the samples have been compressed starting from (a) →(b) →(c) →(d).

3.5 SINTERING PROFILE

Sintering is a high temperature heat treatment process which promotes consolidation as well as densification in a compacted powdered substance. This concurrently changes the chemical composition, phase composition, particle size and shape of re powdered substances as the sintering temperature increases. The sintering process begins with the formation of necks between particles in the green part up to an approximate density of 65%. This is followed by the intermediate stage which is generally the stage where the pores in the compact become isolated, leading to an increase in relative density up to approximately 90%. In the last stage, the elimination of pores takes place resulting in a near fully dense ceramic. During sintering, the initial powdered compact shrinks to attain its highest bulk density (Champoin, 2013).

3.6 GRINDING AND POLISHING

Prior to microstructural evaluation, Vickers hardness and fracture toughness measurement of the sintered samples, grinding and polishing process were first carried on the sintered samples were ground and polished on one of its surface using a grinding and polishing machine (Metapol-2, scientific Technologies). The sintered samples were surface ground manually using silicon carbide (SiC) sandpapers with a grit size varying from 600-1200.

3.7 Characterization

The characterization process includes the X-Ray diffraction (XRD) for HA powders; Fourier Transform Infrared (FTIR), Scanning Electron Microscopy (SEM) with Energy Dispersive X-Ray (EDX) analysis for additive samples followed by grain size evaluation (SEM) and Vickers hardness for all the HA additive sintered samples.

3.7.1 Fourier Transformation Infrared (FTIR)

A Fourier transform infrared spectrometer (FTIR – Brukers IFS-66-VS, Germany) with a reflectance mode was used for qualitative analysis of the molecular radicals. Prior to testing, 40 mg of KBr is mixed with 0.4 mg of the tested powder. Subsequently, sample powder is pressed into pellet of 13 mm in diameter. Advanced preparation is not required for the sintered samples. The possible structural variation and reactions in those samples were examined. The infrared spectrum with a resolution of 4 cm^{-1} and a scan number of 32 was adopted with a scan range $400 - 4000$ cm^{-1}.

3.7.2 Scanning Electron Microscopy (SEM) and Energy Dispersive X-Ray Analysis (EDX)

The morphology, the Ca/P ratio and the distribution of elemental within the HA powder and sintered samples were examined on a phenom Pro-X microscope equipped with an energy dispersive X-Ray (Pro Suite & Elemental Analysis, Phenom). Measurements were made in terms of atomic %, weight % and elemental spectra acquisition.

3.7.3 X-Ray Diffraction (XRD)

X-ray diffraction (XRD) provides information that relates to the crystal lattice of the material and can characterize the crystalline phases present. In the present work, the phases present in the powders as well as the sintered samples were determined at room temperature

using X-Ray diffraction (Empyrean, PANalytical, Netherlands) operated at 35 kV and 15 mA with Cu-Kα as the radiation source. The X-ray scan speed and step scan were 0.5°/min. and 0.02°, respectively.

3.7.4 Bulk Density Measurement

The bulk densities of dense compacts (above 90% of theoretical density) were determined by the water immersion technique based on the Archimedes principle using a standard AD-1653 from A&D company limited. In the present research, distilled water was used as the immersion medium. The procedure to measure the bulk density can be summarized as follows:

(a) The dry weight of the sample is first measured.

(b) The sample is placed on a dish immersed in the distilled water after the electronic balance is zeroed. The weight of the sample in water is subsequently recorded. Extra care has to be taken, as any minor disturbance will incur vibration causing the readings to fluctuate.

The bulk density was calculated using equation below:

$$p = \frac{W_a}{|W_a - W_w|} \times p_0$$

Where ρ is the bulk density of sample (g/cm^3), W_a is the weight of the sample in air (g), W_w is the weight of the sample in water (g) and ρo is the density of distilled water. The temperature effect on the density of distilled water was taken into consideration using the table provided in Appendix. However, for low-density samples (below 90% of theoretical density) the bulk density was obtained from the measurement of geometric dimensions and

sample mass. This is because the former method allows water to penetrate the pores, resulting in an overestimate value of the sample's density.
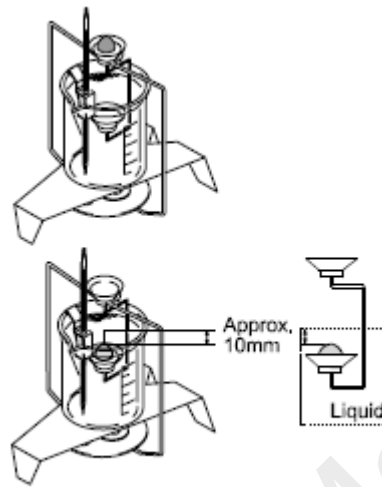
Figure 3.6 Weight balance to measure weight and submerged weight.

3.7.5 Vickers Hardness and Fracture Toughness Evaluation

The Vickers hardness testing method was used to ascertain the hardness of the sintered HA. The indentations were made using a pyramidal diamond indenter (HMV series Shimadzu, Japan) with an applied load varying from 50 g to 200 g. In the Vickers test, the load is applied smoothly, without impact, and held in place for 10 seconds. The physical quality of the indenter and the accuracy of the applied load are defined clearly in ASTM E384-99 (1999) and must be controlled to get the correct results. In general, the Vickers indentation (Figure 4.9) appears to be square, and the two diagonals have almost the same lengths. After the load is removed, the indentation diagonals as shown in Figure 4.9 are measured usually with a filarmicrometer built in the attached microscope on the Vickers machine, to the nearest 0.1 μm and the average value, *2a*, is obtained. The Vickers hardness (*Hv*) is calculated based on the surface area of the indent using the equation below:

$$H_v = \frac{1.854P}{(2a)^2}$$

Where *P* is the applied load and *2a* is the average length of the diagonals. In the present work, five indentations were made for each sample and the average values were taken.
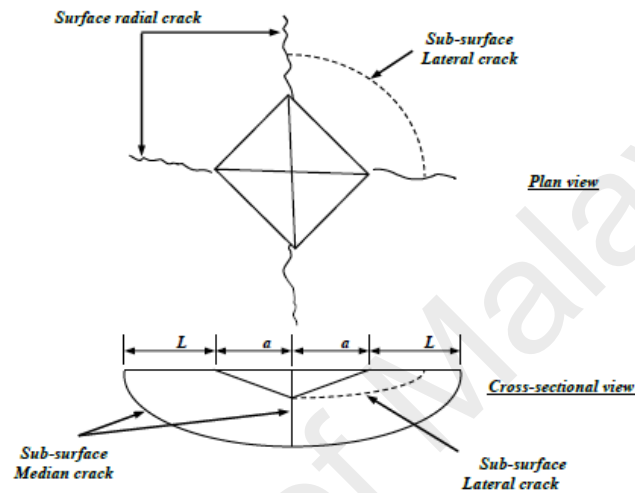
Figure 3.7. Schematic indentation fracture pattern of an idealized Vickers median (or half penny) crack system (Niihara et al., 1982)

Figure 3.8: Above diagram show the diagonal after the indentations from machine.

Using the same indentation image from Vickers hardness tester, fracture toughness (K*Ic*) was determined from the equation derived by Niihara (1985):

$$K_k = 0.203 \left(\frac{c}{a}\right)^{-1.5} (H_v)(a)^{0.5}$$

Where *Hv* is the Vickers hardness, *c* is the characteristics crack length (L+a), *L* is the average crack length and *a* is the half diagonal of indent.

CHAPTER 4: RESULTS AND DISCUSSION

4.1 Calcium Precursor Analysis
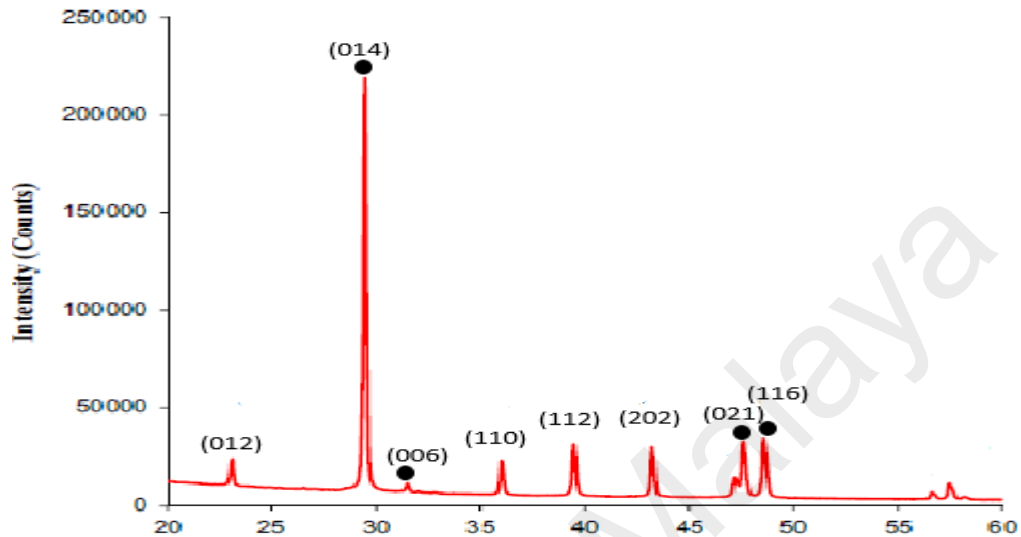
Figure 4.1: The XRD diffractogram of the crushed eggshells. All the peaks belong to $CaCO_3$.

The XRD diffractogram of crushed eggshells is show in Figure 4.1 above. Predominant peaks of $CaCO_3$ are observed in the structure of crushed eggshells where the highest intensity peak is observed data 2θ angle of 29.51 corresponding to a Miller indices of (104). From Elizondo et al., (2012) reported the decomposition of $CaCO_3$ to CaO from the raw material eggshell has been reported at a low calcination temperature of 700°C and others between 830 and 850°C (Ho et al., 2013 and Dasgupta et al., 2004). Other than that, Chaudhuri et al., 2013 and Goloshcapov et al., 2013) reported that temperature at 900°C found the decomposition of $CaCO_3$ to CaO while 1000°C from Dahlan et al., 2012 and Raihana et al., 2008). Hence, the calcination temperature was chosen in a temperature range of 700–1000°C for the current study. Figure 4.2 shows the XRD patterns of CaO produced from crushed eggshells at different calcination temperatures. Upon calcination of eggshells at 850, 900, and 1000°C, the XRD results indicate only the crystalline phase formation of

CaO. However, calcination results at 700 and 800°C observed the presence of both $CaCO_3$ and CaO. This indicates an incomplete transformation of the $CaCO_3$ in eggshells to CaO. The highest intensity CaO peak is observed data at a 2θ angle of 37.31 corresponding to the (200) lattice plane. At different calcination temperatures the intensity of the strongest CaO peak increased from 850°C to 900°C, followed by a drop at 1000°C. The highest crystallinity was obtained at 900°C. Therefore, the calcination temperature of eggshells was set at 900°C.
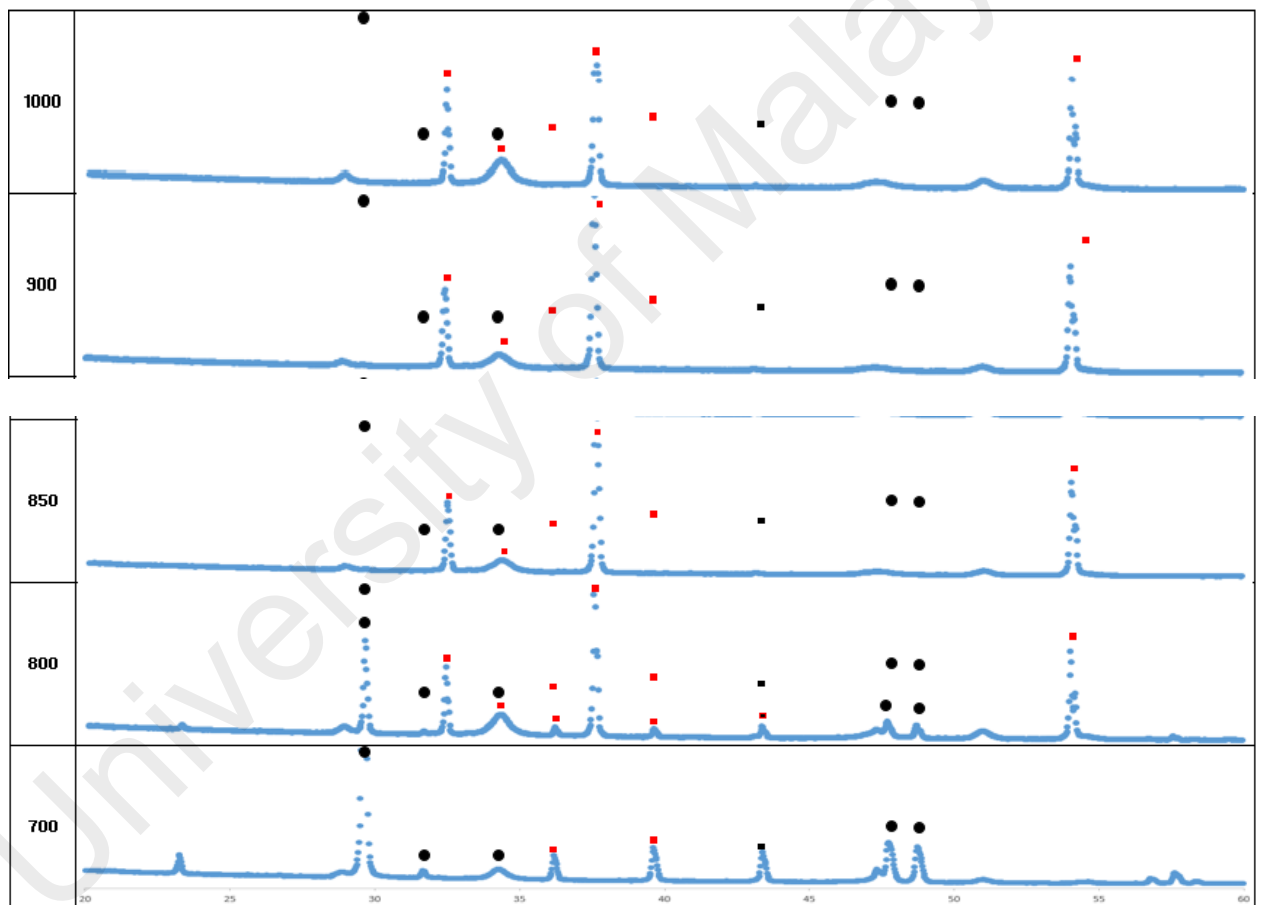
Figure 4.2: The XRD diffractograms of the CaO produced via calcination at different temperatures.

4.2 Relative Density of Undoped and additive doped Sintered HA

The densification curves of undoped and additive doped HA as a function of sintering temperatures are shown in Figure 4.3. The relative density of pure HA decreased when the sintering temperature exceeded 1150°C.

However, the bulk density for additive doped HA increased with increasing temperature up to 1350°C. From Figure 4.3, it is noticeable that ZnO-doped HA samples have demonstrated higher densification than pure HA as all the doped samples attained high relative density > 99% at 1250°C while pure HA could obtain only 90% of the theoretical density at the same temperature. On the other hand, the sintering study showed that 1250°C is the optimum sintering temperature in densifying Zn-doped HA while all the other doped samples attained their highest relative density at 1350°C except for pure HA. Pure HA attained a highest density of 92% at 1150°C.
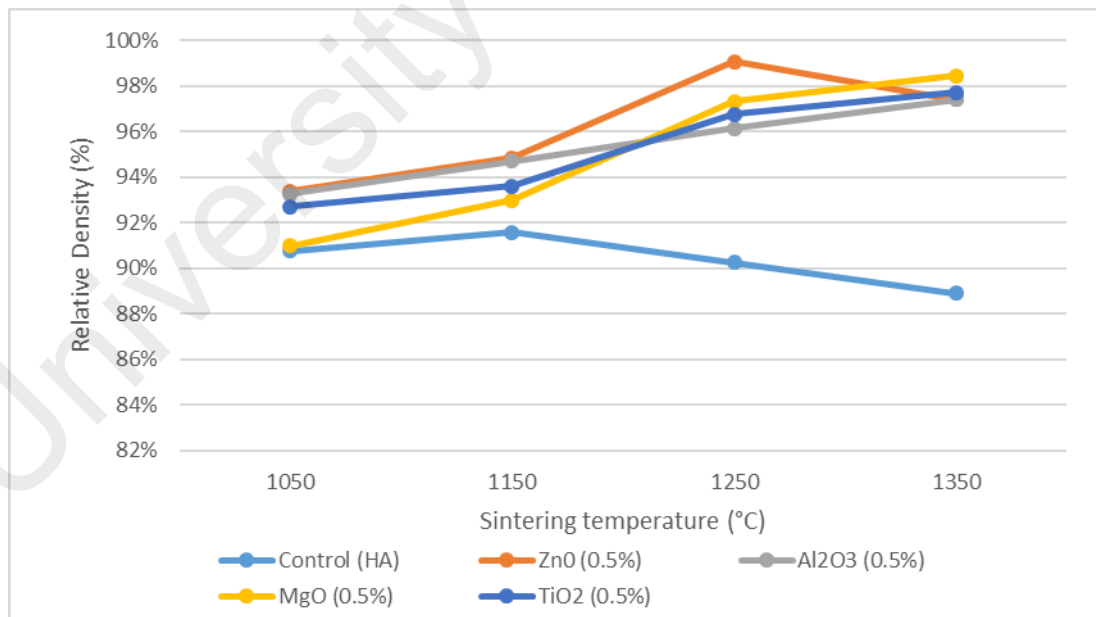
Figure 4.3: Relative density variation as a function of sintering temperatures for HA with different addition chemical.

Besides, it also appeared that 0.5 wt% ZnO amount is beneficial for the densification of HA especially at high temperature of 1250°C as shown in Figure 3 followed by MgO (97%), TiO_2 (97%) and Al_2O_3 (96%). While for 1350°C, MgO and TiO_2 improved 1 percent to 98% while ZnO and Al_2O_3 achieve around 97%. This could be due to addition of ZnO enhanced the mass transport through the grain boundaries and thus lead to higher final densities. Moreover, zinc oxide was found to be beneficial in enhancing the densification of HA when compared to other sintering additives such as silver, iron and titania (Bhattacharjee et al., 2011; Kramer et al., 2013; Wang and Chaki., 1994).

4.3 Vickers Hardness of undoped and Additive-doped Sintered HA

The beneficial effect of doped of additive in improving the hardness of HA has been revealed. It could be perceived that at temperatures from 1050°C to 1250°C, all the additive doped HA samples demonstrated a hardness superior to that of undoped HA.

Table 1: A comparison of optimum Vickers hardness between undoped and doped additive sintering.

Additive concentration (0.5 wt%)	Maximum Vickers Hardness (GPa)
Control (HA)	4.95
Zn0	6.59
Al_2O_3	7.551
MgO	6.295
TiO_2	7.041
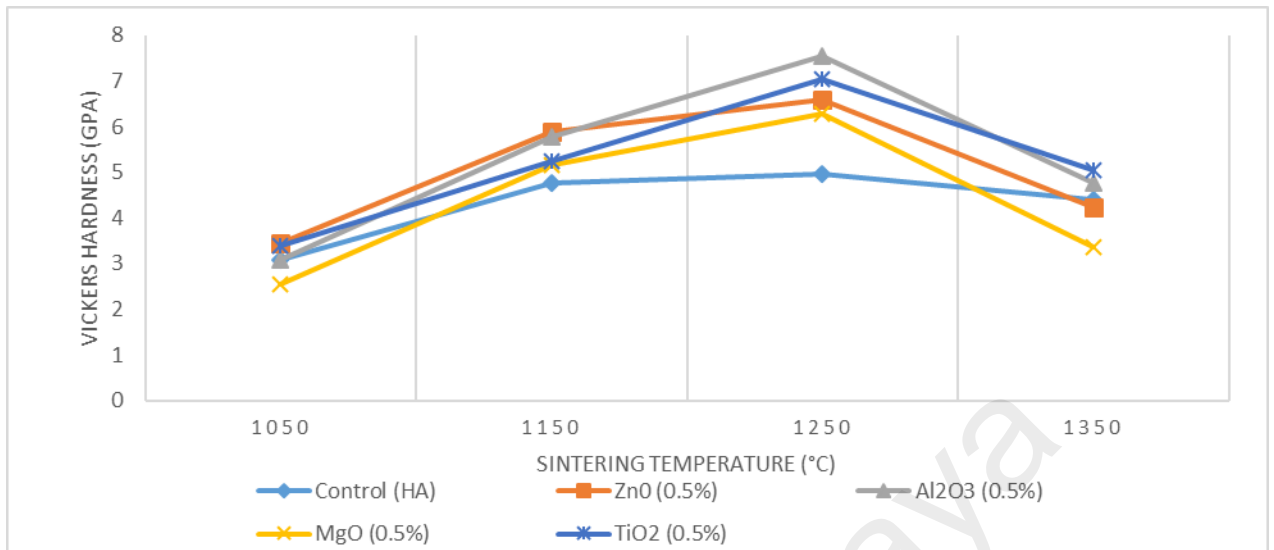
Figure 4.4: Effect of sintering temperature and additive addition on the Vickers hardness of HA.

The maximum hardness achieved for all additive-doped and undoped HA is summarized in Table 1. In short, all type of additive samples were found to be most effective and obtained highest hardness at temperature 1250, even undoped HA also showed the highest at 1250°C.

The effects of addition additive and sintering temperature on the Vickers hardness of sintered HA are shown in Figure 4.4. A general observation which can be made from Figure 4.4 is that the measured hardness of all the undoped and additive chemical-doped HA revealed a similar trend where the hardness increases with increasing temperature, consequently reaching the maximum hardness value at certain temperature; followed by a decrease with further increase of sintering temperature. For example, the hardness of Aluminum oxide (Al_2O_3) doped HA peaked at 1250°C (7.551GPa) and decrease drastically to 4.765GPa at sintering temperature of 1350°C. Meanwhile from the above Figure 4.4. Aluminum oxide showed the highest hardness among other additive chemical at a temperature of 1250°C followed by titanium oxide, zinc oxide, magnesium oxide and last is hydroxyapatite. This increase in hardness may have been due to inherent characteristics of

the aluminum oxide (Al_2O_3). Al_2O_3 possesses strong ionic interatomic bonding, giving rise to its desirable material characteristics, such as hardness and strength. The most stable hexagonal alpha phase Al_2O_3 is the strongest and stiffest of the oxide ceramics (Ellakwa et al., 2008). Other than that, study of addition of Al_2O_3 by Choi and his colleagues (1998) on hydroxyapatite also proves the increase in strength due to the formation of a strong bond between HAp and Al_2O_3 without microcracks. Biocompatibility study between alumina oxide with hydroxyapatite from Jorge et al (2009), the optimum of alumina oxide via plama spray, the biocompatibility of the coating remained unaltered, as Al_2O_3 retained its bio-inertness. Another biocompatibility from Lee and his colleagues (2014), hydroxyapatite with the addition of alumina oxide showed increased activity and Ca ions were observed to have been produced.
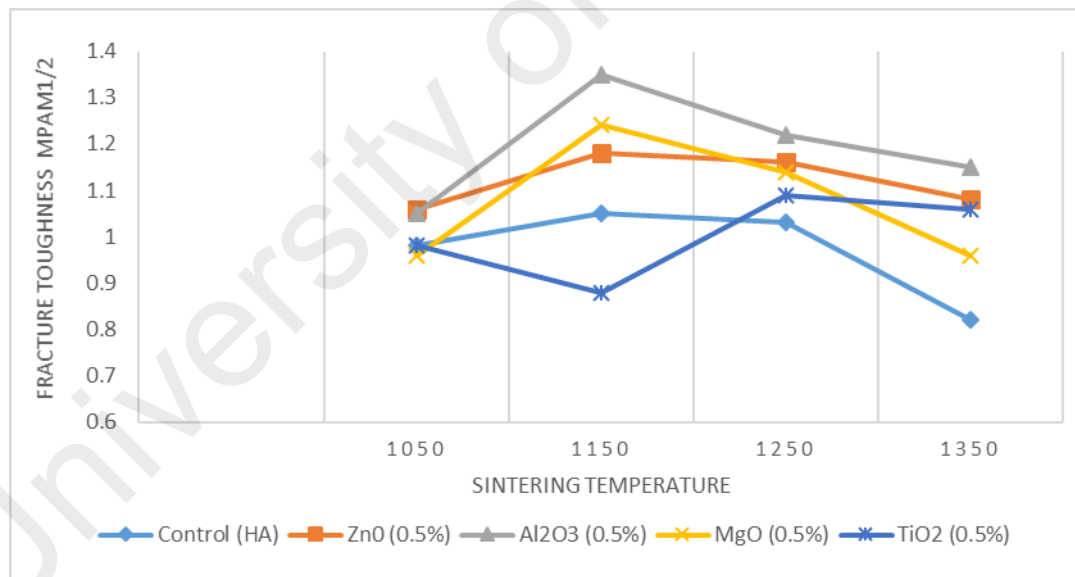
Figure 4.5: Effect of sintering temperature and additive sintering on the fracture toughness of HA.

Figure 4.5 shows the effect of sintering temperature between all additives sintering on the fracture toughness. From the figure 4.5, undoped HA recorded a fluctuated trend between

fracture toughness and sintering temperature while the Vickers hardness show slightly increase with sintering temperature. At a sintering temperature of 1050°C, low fracture toughness values ($0.96 - 1.06$ MPam$^{1/2}$) were recorded for all the sintered samples which could be attributed to the weak grain boundaries of the HA matrix at low temperature (Champion, 2013)

Further observation indicated the measured fracture toughness of the doped HA revealed a similar trend with Vickers hardness (Figure 4.4) where the fracture toughness increases with increasing temperature, consequently reaching the maximum hardness value at certain temperature; followed by a decrease with further increase of sintering temperature. For example, the fracture toughness of Aluminum oxide (Al_2O_3) doped HA peaked at a maximum value (1.35 MPam$^{1/2}$) when sintered at 1150°C and decreased almost linearly with increasing temperature (>1150°C). Similarly, for Magnesium oxide (MgO) also sharing the similar trend where it achieved highest toughness (1.24MPam$^{1/2}$) and decrease when the sintering temperature increase.

From Figure 4.5, at a sintering temperature of 1350°C, low fracture toughness values were recorded for all the samples. Based on Buys et al. (1995), HA decomposition to secondary phase (TCP) is one of the root causes to explain the reducing of mechanical properties of HA when the temperature exceeds more than 1200°C. The volume changes associated with the formation of these new secondary phases creates internal strain within the HA matrix.

CONCLUSION

The present study aims at synthesizing and investigating the sinterability of phase pure hydroxyapatite (HA) via wet chemical precipitation route, using waste eggshells as a calcium precursor. The beneficial effect of adding additive sintering on the HA particularly on the hardness and fracture toughness has also been evaluated. The following conclusions can be drawn:

1) Prior to the synthesis of EHA, the effects of calcination on the purity of CaO extracted from waste eggshells were investigated, as its usage in the synthesis of high purity HA is of paramount importance. The findings from the aforementioned investigation indicated that at low calcination temperature (700°C and 800°C), $CaCO_3$ inherent in eggshells still remained in the calcined substances. Nevertheless, calcination of eggshells beyond 850°C resulted in the formation of pure CaO with the highest purity attained at 900°C. These results were confirmed via XRD analysis from the calcined substance

2) The bulk density for additive doped HA increases with increasing temperature up to 1350°C. Among all additives, it is noticeable that ZnO-doped HA samples have demonstrated a higher densification which reached until 99%.

3) For the hardness evaluation for all sintering additives, it could be perceived that at temperature from 1050°C to 1250°C, all the additive doped HA samples demonstrated hardness superior to that of undoped HA. The maximum hardness was achieved at a sintering temperature of 1250°C for all the additives. When the temperature reached 1350°C, the hardness showed reduction. This suspected due to decomposition of HA to its secondary phases (α-TCP and TTCP),hence reduce its performance. The

decomposition of HA to its secondary phases can be investigated in a future for coming study via XRD.

Apart from its ability to produce high purity HA along with good mechanical properties, the usage of eggshells in the synthesis of HA was an inexpensive alternative to commercial available calcium precursors. Its usage also promotes the reduction of green waste that we daily generated. Other than that, the doped additive show that in terms of mechanical properties and density, the doped show better than pure hydroxyapatite. In conclusion, the objectives of the research that were mentioned in chapter 1 were achieved.

Future Work

Following are some suggestions for further work to be done:

1. To be able thoroughly evaluate the aptness of additive sintering with hydroxyapatite as bone implant materials, future research should incorporate in-vitro and in vivo analysis.

2. Evaluate different amount of doped sintering and compare its mechanical and physical properties.

3. The use of more sophisticated equipment such as transmission electron microscope (TEM) could be used to investigate the structure and capture the image as SEM faced limitation when unable capture the clear image.

4. The faster sintering method like microware can be study as sintering under conventional furnaces took more time.

5. Study phase purity and phase decomposition at higher sintering temperature.

REFERENCES

Ahmed, S. Ahsan, M. (2008). Synthesis of Ca-hydroxyapatite bioceramic from egg shell and its characterization. Bangladesh Journal of Scientific and Industrial Research, 43(4), 501-512

Alomary, A.,Belhadj, S., Obeidat, S., Al-Momani, I., & Attiyat, A. (2012). A comparison of SEM-EDS with ICP-OES for the Quantitative Elementa Determination of Algerian Mediterranean Sea Sediments. *Jordan Journal of Chemistry*

AMinatun, Siswanto, Penga, Y.,Istifarah,& Apsari,R. (2013). The effect of Sintering Process on the Characteristics of Hydroxyapatite from Cuttlefish Bone (Sepia Sp.) *Research Journal of Pharmaceutica, Biological, and Chemical Sciences* 4(4), 1431-1442

Balasundaram,G., Sato, M, M., and Webster, T.J. (2006). Using hydroxyapatite nanoparticles and decreased crystallinity to promote osteoblast adhesion similar to functionalizing with RGD. *Biomaterials*, 27(14), 2798-2805

Balazsi,K.,Sim,h.Y.,Choi, J.Y.,Kim, S.G.,Chae,C.H.,and Balazsi, C. (2013). Biogenic Nano sized Hydroxyapatite for tissue Engineering Application. 38, 190-193

Bardhan, R., Mahata, S., and Mondal, B. (2011). Processing of natural resourced hydroxyapatite from eggshells waste by wet precipitation method. *Advances in Applied Ceramic*, 110(2), 80-86

Best,A., Cojazzi, G., panzavolta, S., Ripamonti, A., Roveri, N., Romanello, M., Moro, L. (1997). Chemical and structural Characterization of the Mineral phase from cortical and Trabecular Bone. *Journal of Inorganic Biochemistry*, 68, 45-51

Best, S., Porter, A., Thian, E., and Huang, J. (2008). Bioceramics: Past, present and for the future. *Journal of the European Ceramic Society, 28*(7): 1319-1327.

Bureau.M. N., Denault, J., and Legoux, J.G (2006) Implantable biomimetic prosthetic bone: Google Patents

Buys, A., Sorrell, C., Brandwood, A., and Milthorpe, B. (1995). Hydroxyapatite sintering characteristics: Correlation with powder morphology bv high-resolution microscopy. *Journal of materials science letters, 14*(10): 744-747.

Catros, S., Guillemot, F.,Lebraud, E., Chanseau, C.,Perez, S., Bareille, R., Fricainm J.C. (2010). Physico-chemical and biological properties of a nano- hydroxyapatite powder-chemical powder synthesized at room temoerature. *IRBM*, 31(4), 226-233

Champion, E. (2013). Sintering of calcium phosphate bioceramics. *Acta biomaterialia, 9*(4): 5855-5875.

Champion, E., Gautier, S., and Bernache-Assollant, D. (1996). Characterization of hot pressed Al_2O_3-platelet reinforced hydroxyapatite composites. *Journal of Materials Science: Materials in Medicine, 7*(2): 125-130.

Chaudhuri, b.,Mondal, Modak , D.K Pramanik, K,and Chaudhuri, B.K.(2013). Preparation and characterization of nanocrystalline hydroxyapatite from eggshell and K$_2$HPO*4* solution. *Materials Letters*, 97, 148-150

Dahlan, K.,Dewi, S. U., Nurlaila, A., & Soejoko, D. (2012). Synthesis and Characterization of calcium Phosphate/ Chitisan Composites. *International Journal of Basic &Applied Science*, 12(1), 50-57.

Dasgupta, P.,Singh, A., Adak,S.,and Purohit, K.(2004), Synthesis and characterization of hydroxyapatite produced from eggshell. Paper presented at the International Symposium of Research Students on Materials Science and Engineering.

Doremus, R. (1992). Bioceramics. *Journal of Materials Science, 27*(2): 285-297.

Dorozhkin, S.V. (2009). Calcium orthophosphate cements and concretes. *Materials, 2*(1): 221-291.

Dorozhkin, S.V. (2010). Calcium orthophosphates as bioceramics: State of the art. *Journal of functional biomaterials, 1*(1): 22-107.

Elizondo-Villarreal, N., Martinez-de-la-Cruz, A.,Guerra, R.O., Gomez-Ortega, J.L., Torres-Martinez, L. M., & Castano, V.M. (2012). Biomaterials from Agricultural Waste: Eggshells- based Hydroxyapatite. *Water, Air& Soil Pollution*, 223(7), 3643-3646

Fathi,M.H., Mortazavi,V.,and Roohani Esfahani, S.I.(2009) Bioactivity Evaluation of Synthetic Nanocrystalline Hydroxyapatite. *Dental Research Journal*, 5(2).

Ferraz, M.,Monteiro, F., and Manuel, C.(2004)Hydroxyapatite nanoparticels: A review of preparation mythologies. *Journal of Applied Biomaterials and Biomechanics*

Feng,W., mu-sen,L., Yu-Peng, L., &Yong-xin, Q. (2005). A simple sol gel technique for preparing hydroxyapatite nano-powders. *Materials Letters*, 59(8-9), 916-919

Gergely,G.,Weber,F.,Lukacs, I., Toth, A Horvath, Z.E.,Mihaly, J.,and Balazsi,C.(2010). Preparation and characterization of hydroxyapatite from eggshell. *Ceramics International*, 36(2), 803-806.

Goloshchapov, D.L., Kashkarov V.M, Rumyantseva N.A. Seredin P.V., Lenshin,A. S., Agapov, B.L. . Domashevskaya, E.P. (2013) Synthesis of nano- crystalline hydroxyapatite by precipitation using hen's eggshell, *Ceramic International* 39(4)4539–4549.

Ho, W.-F., Hsu, H-c., Hsu, S-K., Hung, C-W., and Wu, S.-C (2013). Calcium phosphate bioceramic synthesized from eggshell powder through a solid state reaction. *Ceramic International*, 39(6), 6467-6473.

Hench, L.L. (1991). Bioceramics: From concept to clinic. *Journal of the American Ceramic Society, 74*(7): 1487-1510.

Hui,P., Meena, S.,Sign, G., Agarawal, R.,and Prakash ,S.(2010). Synthesis of Hydroxyapatite Bio-Ceramic Powder by Hydrothermal Method. *Journal of Materials & Materials Characterization and Engineering*, (8), 683-692.

Ibrahim,_a,-R.,Wei, W., Zhang, D., Wang, H., and Li, J (2013). Conversion of waste eggshells to mesoporous hydroxyapatite nanoparticles with high surface area. *Materials Letters*, 100,195-197

Jayaswal, G.P., Dange, S., and Khalikar, A. (2010). Bioceramic in dental implants: A review. *The Journal of Indian Prosthodontic Society, 10*(1): 8-12.

Kbari, B., Tavandashti, M.P., and Zandrahimi, M. (2011). Particle size characterization of nanoparticles- A practical approach. *Iranian Journal of material Science and Engineering*, 8(2), 48-56

Kehoe, S.(2008). Optimisation of hydroxyapatite (HAp) for orthopedic allocation via the chemical precipitation technique. Doctoral dissertation, Dublin City University.

Kim, H.W., Kong, Y.M., Koh, Y.H., Kim, H.E., Kim, H.M., and Ko, J.S. (2003). Pressureless sintering and mechanical and biological properties of fluor-hydroxyapatite composites with zirconia. *Journal of the American Ceramic Society, 86*(12): 2019-2026.

Krishna, D.S.R., Siddharthan, A., Seshadri, S.K., and Sampahth Kumar, T.S.(2007). A novel route for synthesis of nanocrystalline hydroxyapatite from eggshell waste. *Journal of Materials Science: Materials in Medicine*, 18(9),1735-1743.

Kutty, M.G., and Singh, R. (2001). The effects of zirconia additions on the sintering behaviour and phase stability of hydroxyapatite ceramics. *Pertanika Journal of Science & Technology, 9*(2): 229-238.

Kumar,G.S., Thamizhavel, A., Girija, E.K (2012). Microware conversion of eggshells to flower like hydroxyapatite nanostructure for biomedical applications. *Materials Letters*, 76,198-200

Kumar,G.S., &Girija, E.K.(2013). Flower like hydroxyapatite nanostructure obtained from eggshells: A candidate for biomedical applications. , 39(7), 8293-8299

Lee, S.J., and Oh, S.h. (2003). Fabrication of calcium phosphate bioceramic by using eggshell and phosphoric acid. *Materials Lette*rs, 57(29), 4570-4574

Li, C. (2009). Crystalline behaviors of hydroxyapatite in the neutralized reaction with different citrate additions. *Powder Technology*, 192(1), 1-5

Luo,P.,and Nieh, T.(1995). Synthesis of ultrafine hydroxyapatite particles by a spray dry method. *Materials Science and Engineering*: C, 3(2), 75-78

Mostafa, N. Y. (2005). Characterization, thermal stability and sintering of hydroxyapatite powders prepared by different routes. *Material chemistry and Physics*, (4(2-3)), 333-341

Mostafa, N. Y. (2005) characterization, thermal stability and sintering of hydroxyapatite powder prepared by different routes. *Materials Chemistry and Physics*, 94(2-3), 333-341

Nayak, A.K. (2010). Hydroxyapatite Synthesis Methologies: An Overview International Journal of ChemTech research, 2(2)

Okada, M., and Furuzono, T. (2006). Calcination of Rod-like hydroxyapatite Nanocrystals with an Anti-sintering Agent Surrounding the Crystals. *Journal of Nanoparticles Research*, 9(5), 807-815

Oktar, F.N., Agathopoulos, S., Ozyegin, L.S., Gunduz, O., Demirkol, N., Bozkurt, Y., and Salman, S. (2007). Mechanical properties of bovine hydroxyapatite (bha) composites doped with sio2, MgO, Al$_2$O$_3$, and ZrO$_2$. *Journal of Materials Science: Materials in Medicine, 18*(11): 2137-2143.

Orlovskii, V.,Komlev,V.,and Barinov, S.(2002). Hydroxyapatite and hydroxyapatite based ceramic. *Inorganic Materials*, 38(10), 973-984

Padmanabhan, S.K., Ui Hap, E., Licciulli, A. (2014). Rapid synthesis and characterization of silicon substituted nano hydroxyapatite using microwave irradiation. *Current Applied Physics*, 14(1), 87-92.

Paz, A.,Guadarrama, D.,Lopez, M.,E Gonzalez, J.,Brizuela, N., and Aragon, J. (2012). A comparative study of hydroxyapatite nanoparticles synthesized by different routes. *Quimica Nova*, 35(9), 1724-1727

Prabakran,K., Balamurugan, A., and Rajeswari, S.(2005). Development of calcium phosphate based apatite from hens eggshell. *Bulletin of Materials Science*, 28(2), 115-119

Prabakaran, K., and Rajeswari, S. (2009). Spectroscopic investigations on the synthesis of nano-hydroxyapatite from calcined eggshells by hydrothermal method using cationic surfactant as template. *Spectrochimica Acta Part A: Molecular and Bimolecular Spectroscopy*, 74(5), 1127-1134

Qiu,C., Xiao, .X, and Liu, R. (2008). Biomimetic synthesis of spherical nano-hydroxyapatite in the presence of polyethylene glycol. *Ceramics International*, 34(7), 1747-1751

Rao, R.R., and Kannan, T. (1999). Synthesis and sintering of hydroxyapatite in presence of oxide additives. *Transactions of the Indian Ceramic Society, 58*(3): 64-68.

Ramesh, S., Tan, C., Bhaduri, S., and Teng, W. (2007a). Rapid densification of nanocrystalline hydroxyapatite for biomedical applications. *Ceramics international, 33*(7): 1363-1367.

Ramesh, S., Tan, C., Peralta, C., and Teng, W. (2007b). The effect of manganese oxide on the sinterability of hydroxyapatite. *Science and Technology of Advanced materials, 8*(4): 257-263.

Ramesh, S.,Tan, C.Y., Bhaduri, S.B., Teng W.D. and Sopyan,I.(2008). Densification behavior of nanocrystalline hydroxyapatite bio ceramic. Journal of Materials Processing Technology, 206 (1-3), 221-230

Ramesh, S., Tan, C.Y., Tolouei, R.,Amiriyan. M., Pirbolaksono,J., Sopyan, I., and Teng, W.D. (2012). Sintering behavior of hydroxyapatite prepared from different routes. *Materials & Design*, 34,148-154

Rhee, S.H. and Tanaka, J. (2000). Effect of chlorination sulphate on the crystal growth of hydroxyapatite, *Journal of the American Ceramic Society*, 83(8), 2100-2102

Rho,J-Y.,Tsui, T.Y., and Pharr, G.M. (1997). Elastic properties of human cortical and trabecular lamellar bone measured by Nano indentation. *Biomaterials*, 18(20), 1325-1330.

Rivera, E.M.,Araiza, M., Brostow, W., Castano, V. M., Diaz-Estrada, J., Hernandez, R., and Rodriguez, J.R.(1999) Synthesis of hydroxyapatite from eggshells. *Materials Letters* 41(3), 128-134.

Sadat-Shojai, M., Khorasani, M.-T., Dinpanah-Khoshdargi, E., and Jamshidi, A. (2013). Synthesis methods for nanosized hydroxyapatite with diverse structures. *Acta biomaterialia, 9*(8): 7591-7621.

Sanosh, K.P., Chu, M-C., Balakrishnan, A.,Kim, T.N., &Cho, S-J.(2009). Utilization of biowaste eggshells to synthesize nanocrystalline hydroxyapatite powders. *Materials Letters*, 63(24-25), 2100-2102

Sasikumar,S., and Vijayaraghavan, R. (2006). Low temperature synthesis of nanocrystalline hydroxyapatite from eggshells by combustion method. *Trends in Biomaterials and Artificial Organs*, 19(2), 70-73.

Siddharhan, A., Kumar, T.S.& Seshadri, S.K. (2009), synthesis and characterization of nanocrystalline apatite from eggshells at different Ca/P ratios. *Biomedical Materials*, 4(4), 045010.

Singh, V.and Mehta, N. (2012). Synthesis of Nano Crystalline Hydroxyapatite from Egg shells by Combustion Method. *International Journal of Science and Engineering Investigation*, 1(3), 92-92

Sopyan, I.,Adline, S.F., and Mohamad, S.A. (2011). Preparation of Dense Biphasic Calcium Phosphate Ceramic Using Eggshell Derived Nanopowders. *Applied Mechanic and Materials*, 110-116, 3645-3649

Siddarthan,A., Kumar,T.S., and Seshadri, S.K. (2009) Synthesis and characterization of nanocrystalline apatite from eggshell at different Ca/P ratios. *Biomedical Materials*, 4(4), 045010

Smolen,D.,Chudoba, T.,Gierlotka,SKedzierska,A Lojilowski, W., Sobczak,K., Kurzydlowski,K.J (2012).Hydroxyapatite Nano powder Synthesis with a Programmed resorption Rate. *Journal of nanomaterials*, 2012, 1-9

Suchanek, W., Yashima, M., Kakihana, M., and Yoshimura, M. (1997). Hydroxyapatite ceramics with selected sintering additives. *Biomaterials, 18*(13): 923-933.

Tolouei, R., Tan, C., Amiriyan, M., and Teng, W. (2011). Sintering effects on the densification of nanocrystalline hydroxyapatite. *Int J Automot Mech Eng (IJAME), 3*: 249-255.

Vallet-Regi, M.(2001). Ceramics for medical applications. *Journal of chemical Society, Dalton Transactions* (2) ,97-108

Vallet-Regi, M., and González-Calbet, J.M. (2004). Calcium phosphates as substitution of bone tissues. *Progress in Solid State Chemistry, 32*(1): 1-31.

Wang, P.E., and Chaki, T. (1993). Sintering behaviour and mechanical properties of hydroxyapatite and dicalcium phosphate. *Journal of Materials Science: Materials in Medicine, 4*(2): 150-158.

Wang,P.,Li,C., Gong, H., Jiang, X., Wang, H.,and Li,K.(2010). Effect of synthesis conditions on the morphology of hydroxyapatite nanoparticles produces by wet chemical process. *Powder Technology*, 203(2), 315-321.

Wu, S.-C Tsou, H-K., Hsu, H-C., Hsu, S-K.,Liou, S-P., and Ho, W.-F.(2013).A hydrothermal synthesis of eggshell and fruit waste extract to produce nanosized hydroxyapatite. *Ceramic International*, 39(7), 8183-8188

Xu, J., Khor, K.A., and Kumar, R. (2007). Physicochemical differences after densifying radio frequency plasma sprayed hydroxyapatite powders using spark plasma and conventional sintering techniques. *Materials Science and Engineering: A, 457*(1): 24-32.

Xue,W., Tao, S., Liu, ,X.,Zheng,X., and Ding ,C.(2004). In vivo evaluation of plasma sprayed hydroxyapatite coating having different crystallinity. *Biomaterials*, 259(3), 415-421.

Yang, D.A.,Yang, Z.,Li,X.,Di, L-Z., and Zhao, H. (2005). A study of hydroxyapatite. Calcium sulphate bio ceramic. *Ceramic International*, 31(7), 1021-1023.

Zhang, H-B., Zhou, K-C., Li,Z-Y., and Huang, S-P.(2009). Plate like hydroxyapatite nanoparticles conversion in gastropod (abalone) Nacre. *Chemistry of Solid*, 70(1), 243-248

Zhang , X., and Vecchio, K.S. (2006). Creation of dense hydroxyapatite (synthetic bone) by hydrothermal conversion of seashells. *Materials Science and Engineering*: C, 26(8), 1445-1450

Zhang , Y.,Lu, J., Wang, Yang, S., and Chen , Y. (2009). Synthesis of nano-rod and needle like hydroxyapatite crystal and role of pH adjustment. *Journal of Crystal Growth*, 311(23-34), 4740-4746.

Zhou, H., and Lee, J. (2011). Nanoscale hydroxyapatite particles for bone tissue engineering. *Acta Biomaterialia, 7*(7): 2769-2781.

Zhu,R., Yu, R., Yao, J., Wang, D., and Ke, J. (2008). Morphology control of hydroxyapatite through hydrothermal process. *Journal of Alloys and Compounds*, 457 (1-2), 555-559.

Zhang , Y.,Lu, J., Wang, Yang, S., & Chen , Y. (2009). Synthesis of nanorod and needle like hydroxyapatite crystal and role of pH adjustment. Journal of Crystal Growth, 311(23-34), 4740-4746.